Sources and Transformations of Anthropogenic Nitrogen along an Urban River-Estuarine Continuum

Michael J. Pennino[1,a,*], Sujay S. Kaushal[1], Sudhir Murthy[2], Joel Blomquist[3], Jeff Cornwell[4], and Lora Harris[5]

[1]Department of Geology and Earth Systems Science Interdisciplinary Center, University of Maryland, College Park, MD, USA.

[2]DC Water, Washington, DC, USA.

[3]U.S. Geological Survey, Baltimore MD, USA.

[4]Center for Environmental Science, University of Maryland Horn Point Laboratory, Cambridge, MD, USA.

[5]Center for Environmental Science, University of Maryland Chesapeake Biological Laboratory, Solomons MD, USA.

[a]Now at: US EPA, Office of Research and Development, National Health and Environmental Effects Research Laboratory, Corvallis, OR 97333, USA.

*Corresponding author email: michael.pennino@gmail.com,

Abstract

Urbanization has altered the fate and transport of anthropogenic nitrogen (N) in rivers and estuaries globally. This study evaluates the capacity of an urbanizing river-estuarine continuum to transform N inputs from the world's largest advanced (e.g. phosphorus and biological N removal) wastewater treatment facility. Effluent samples and surface water were collected monthly along the Potomac River Estuary from Washington D.C. to the Chesapeake Bay over 150 km. In conjunction with box model mass balances, nitrate stable isotopes and mixing models were used to trace the fate of urban wastewater nitrate. Nitrate concentrations and $\delta^{15}N\text{-}NO_3^-$ values were higher down-estuary from the Blue Plains wastewater outfall in Washington D.C. (2.25±0.62 mg/l and 25.7±2.9‰, respectively) compared to upper-estuary concentrations (1.0±0.2 mg/l and 9.3±1.4‰, respectively). Nitrate concentration then decreased rapidly within 30 km down-estuary (to 0.8±0.2 mg/l) corresponding with an increase in organic nitrogen and dissolved organic carbon, suggesting biotic uptake and organic transformation. TN loads declined down-estuary (from an annual average of 48,000±5,000 kg/day at the sewage treatment plant outfall to 23,000±13,000 kg/day at the estuary mouth), with the greatest percentage decrease during summer and fall. Annually, there was a 36±19% loss in wastewater NO_3^- along the estuary, and 4–71% of urban wastewater TN inputs were exported to the Chesapeake Bay, with the greatest contribution of wastewater TN loads during the spring. Our results suggest that biological transformations along the urban river-estuary continuum can significantly transform wastewater N inputs from major cities globally, and more work is necessary to evaluate the potential of organic nitrogen and carbon to contribute to eutrophication and hypoxia.

Key Words

Estuary, Mass Balance, Mixing Model, Nitrate Isotopes, Source Tracking, Wastewater

1 Introduction

Urbanization and agriculture have greatly increased the exports of nitrogen from coastal rivers and estuaries globally, contributing to eutrophication, hypoxia, harmful algal blooms, and fish kills (e.g. Aitkenhead-Peterson et al., 2009; Kaushal et al., 2014b; Nixon et al., 1996; Petrone, 2010; Vitousek et al., 1997). Despite billions of dollars spent on regulatory and technological improvements for wastewater treatment plants (WWTPs) and agricultural and urban stormwater runoff (e.g. US-EPA, 1972, 2009, 2011), many coastal waters are still impaired. Also, there are major questions regarding how far urban sources of N (wastewater and stormwater runoff) are transmitted along tidal river-estuarine networks to N-sensitive coastal receiving waters. This study evaluates the capacity of a major river-estuarine system to transform and attenuate N inputs from the world's largest advanced (e.g. phosphorus and biological nitrogen removal) wastewater treatment plant (Blue Plains) before being transported down-estuary to the Chesapeake Bay. We used a combination of stable isotope and box model mass balance approaches to track the fate and transport of anthropogenic nitrogen across space and time.

In addition to urban and agricultural inputs, altered river-estuarine hydrology can contribute to higher exports of N. Jordan et al. (2003) found that annual water discharge increased as the proportion of developed land in a coastal watershed increased. Higher flows, typically during winter and spring months, have also been associated with higher

69 N loads in coastal river-estuaries (Boynton et al., 2008). Furthermore, regional climate
70 variability amplifies pulses of nutrients and other contaminants in rivers (Easterling et al.,
71 2000; IPCC, 2007; Kaushal et al., 2010b; Saunders and Lea, 2008) and alters the biotic
72 transformation of N due to changes in hydrologic residence times (Hopkinson and
73 Vallino, 1995; Kaushal et al., 2014b; Wiegert and Penaslado, 1995). For example, high
74 flow periods related to storms can induce stratification and impact salinity regimes
75 (Boesch et al., 2001), which affects nutrient biogeochemistry like ammonium and
76 phosphate concentrations (Jordan et al., 2008). An improved understanding of the
77 longitudinal assimilatory capacity for nitrogen by large river-estuarine systems across
78 different flow regimes is needed for guiding effective coastal river and estuarine
79 management strategies.

80 One critical and innovative approach to effectively manage coastal nutrient
81 pollution is to 1) track the relative contributions of N export from different sources within
82 the watershed and 2) understand the potential for longitudinal transformation within
83 coastal rivers and estuaries. Recent studies using stable isotopes (Kaushal et al., 2011;
84 Kendall et al., 2007; Oczkowski et al., 2008; Wankel et al., 2006) have shown that these
85 methods can be helpful in elucidating sources and transformations of nitrogen. However,
86 these studies are typically conducted at relatively smaller spatial scales and without
87 coupling to mass balance approaches over both time and space.

88 Here, we combine isotope and mass balance approaches to track sources and
89 transformations of urban wastewater inputs to Chesapeake Bay over space and time
90 across an urban river-estuary continuum spanning over 150 km. The space-time
91 continuum approach has previously been used in studying fate and transport of carbon

and nitrogen in urban watersheds (Kaushal and Belt, 2012; Kaushal et al., 2014c), and here we explore extending it to river and estuarine ecosystems. Our overarching questions were: 1) how does the importance of point *vs.* non-point sources of N shift along a tidal and stratified urban river-estuary continuum across space and time? 2) What is the capacity of an urban river-estuary continuum to transform or assimilate anthropogenic N inputs? 3) How are transport and transformations of N affected by differences in season or hydrology? An improved understanding of how sources and transformations of N change along the urban river-estuarine continuum over space and time can inform management decisions regarding N source reductions along urbanizing coastal watersheds (e.g. Boesch et al., 2001; Kaushal and Belt, 2012; Paerl et al., 2006).

2 Methods

2.1 Site Description

This study is focused on the tidal Potomac River Estuary, which includes the section of the river from Washington D.C. to its confluence with the Chesapeake Bay (Fig. 1). The Potomac River Estuary begins as tidal freshwater, becoming oligohaline ~30-50 km below Washington D.C., and mesohaline at its mouth approximately 160 km below Washington D.C. (Jaworski et al., 1992). The Potomac River Estuary can be seasonally stratified (Hamdan and Jonas, 2006), especially in the southern portion of the system where intruding, saline bottom water from the main stem of the Chesapeake Bay leads to density driven estuarine circulation patterns (Elliott, 1976, 1978; Pritchard, 1956). Mixing is most evident at the estuarine turbidity maximum (Hamdan and Jonas, 2006), ~60-80 km below Washington D.C., and the water column is generally well mixed

114 above the estuarine turbidity maximum zone in the tidal fresh and oligohaline regions of
115 the estuary (Crump and Baross, 1996; Sanford et al., 2001).

116 The watershed draining to the Potomac River Estuary is classified as 58% forested,
117 23% agricultural, and 17% urban, based on Maryland Department of Planning data for
118 2002 (Karrh et al., 2007a). Based on the Chesapeake Bay Program (CBP) Model it was
119 estimated that during 2005 total inputs of nitrogen were 33% from agriculture, 20% from
120 urban (e.g. stormwater runoff and leaky sewers), 19% from point sources (wastewater
121 treatment plants and industrial releases), 11% from forest, 10% from septic, 6 % from
122 mixed open land, and 1 % from atmospheric deposition to water (Karrh et al., 2007b).
123 The CBP model is developed using long-term monitoring data and the non-point loads
124 are estimated from a variety of sources including land cover and agriculture records
125 (Karrh et al., 2007b).

126 The Potomac River Estuary also receives N inputs from the Blue Plains wastewater
127 treatment plant, located in Washington, D.C. In 2009 Blue Plains discharged 2.3 mg/L of
128 NO_3^- and 3.7 mg/L of TN, on average, and exported loads of approximately 2,300 kg/day
129 of NO_3^- and 3,900 kg of TN. Overall, Blue Plains treats and discharges approximately
130 280 million gallons per day (mgd), almost 5% of Potomac River's annual discharge. In
131 the past several decades, Blue Plains has undergone several technological improvements
132 with phosphorus removal in the 1980s and enhanced N removal beginning in the year
133 2000. Since the implementation of advanced wastewater treatment technologies at Blue
134 Plains, there has been a significant decrease ($p < 0.01$) in the concentration of nitrate in
135 effluent discharge, from an average of 7.2 ± 0.3 mg/L before the year 2000 (years 1998
136 and 1999) to an average of 4.1 ± 0.4 mg/L directly after 2000 (years 2001 through 2008).

2.2 Analysis of long-term spatial and temporal water chemistry data

Surface and bottom water N and carbon data collected by the Maryland Department of Natural Resources (DNR) and accessed through the Chesapeake Bay Program's data hub website (Chesapeake Bay Program, 2013) was used to look at historical (1984 to 2012) monthly nutrient concentrations from stations located longitudinally along the Potomac River Estuary (Fig. 1). These data were used to look at the spatial and temporal trends for dissolved and particulate forms of N and dissolved organic carbon (DOC) in the Potomac River Estuary prior to and during this study.

2.3 Water Chemistry Sampling

Water chemistry samples along the Potomac River estuary were collected monthly for one year from April 2010 to May 2011; from 12 km to 160 km below the Blue Plains wastewater treatment plant (See Fig. 1). Water was collected from the surface (top 0.5 m) and bottom water depths. Surface water samplings from 6 km above to 12 km below the Blue Plains wastewater treatment plant effluent outfall were collected seasonally during this time (Fig. 1). Water temperature and salinity was also measured during each water chemistry sampling.

2.4 Nitrate $\delta^{15}N$ and $\delta^{18}O$ Isotope Analyses

Surface samples for $\delta^{15}N\text{-}NO_3^-$ and $\delta^{18}O\text{-}NO_3^-$ isotopes of dissolved nitrate were filtered (0.45 μm), frozen, and shipped to the UC Davis Stable Isotope Facility (SIF) for analysis. The isotope composition of nitrate was measured following the denitrifier

method (Casciotti et al., 2002; Sigman et al., 2001). In brief, denitrifying bacteria are used to convert nitrate in samples to N_2O gas, which is collected and sent through a mass spectrometer for determination of the stable isotopic ratios for N and O of nitrate ($^{15}N/^{14}N$ and $^{18}O/^{16}O$). Values for $\delta^{15}N\text{-}NO_3^-$ and $\delta^{18}O\text{-}NO_3^-$ are reported as per mil (‰) relative to atmospheric N_2 ($\delta^{15}N$) or Vienna Standard Mean Ocean Water (VSMOW) ($\delta^{18}O$), according to $\delta^{15}N$ or $\delta^{18}O$ (‰) = [(R)sample / (R)standard - 1] × 1000, where R denotes the ratio of the heavy to light isotope ($^{15}N/^{14}N$ or $^{18}O/^{16}O$). For data correction and calibration UC Davis SIF uses calibration nitrate standards (USGS 32, USGS 34, and USGS 35) supplied by NIST (National Institute of Standards and Technology, Gaithersburg, MD). The long-term standard deviation for nitrate isotope samples at UC Davis SIF is 0.4 ‰ for $\delta^{15}N\text{-}NO_3^-$ and 0.5 ‰ for $\delta^{18}O\text{-}NO_3^-$. Previous studies (Kaushal et al., 2011; Kendall et al., 2007) indicate that the relative amounts of $\delta^{15}N\text{-}NO_3^-$ and $\delta^{18}O\text{-}NO_3^-$ can be used to determine specific sources of nitrate (i.e. fertilizer, nitrification, atmospheric, or sewage derived nitrate).

It should be noted that while the denitrifier method converts sample NO_3^- and NO_2^- to N_2O gas, in marine systems, NO_2^- has been shown to complicate interpretations of the N and O isotopes of NO_3^- if it remains unaccounted for (e.g. Fawcett et al., 2015; Marconi et al., 2015; Rafter et al., 2013; Smart et al., 2015). This is partially because during the reduction of NO_3^- and NO_2^- to N_2O by the denitrifiers, the O isotope effects are different (and thus need to be corrected for). In addition, the $\delta^{15}N$ of NO_2^- can be extremely different from that of NO_3^-, potentially further complicating interpretation of the data. We found that in the Potomac Estuary stations TF2.1 through LE2.3 (stations from the top of the estuary to the bottom of the estuary) the mean nitrite concentration

183 from 2010-2012 is 0.013 mg/L and the minimum = 0.0055 mg/L and maximum = 0.0183
184 mg/L. The mean nitrite is about 2.4% of the mean nitrate+nitrite concentration. Based
185 on the literature (Fawcett et al., 2015), this level of nitrite is still high enough to have
186 some impacts on the nitrate isotope values, with differences up to 5‰ for both N and O
187 isotopes of nitrate when using the denitrified method with and without nitrite mixed with
188 nitrate in the samples (Casciotti & McIlvin 2007).
189
190 **2.5 Nitrate Isotope Mixing Model**
191 To distinguish between the different potential nitrate sources we used a Bayesian
192 isotope mixing model (Parnell et al., 2010; Parnell et al., 2013; Xue et al., 2012; Yang
193 and Toor, 2016). For the Bayesian isotope mixing model, the Stable Isotope Analysis in
194 R (SIAR) package was used to determine the fraction of nitrate in each sample from four
195 different sources: wastewater, atmospheric deposition, nitrification, and nitrate fertilizer
196 (Parnell et al., 2010; Parnell et al., 2013; Xue et al., 2012; Yang and Toor, 2016). The
197 SIAR mixing model is able to incorporate uncertainty in nitrate source estimates based on
198 the uncertainty in the nitrate source endmembers (Parnell et al., 2010; Parnell et al., 2013;
199 Xue et al., 2012; Yang and Toor, 2016).
200 Nitrate source end-member values, for $\delta^{15}N\text{-}NO_3^-$ and $\delta^{18}O\text{-}NO_3^-$ were obtained
201 from the literature, except wastewater nitrate, which was obtained from this study. The
202 end-member values for $\delta^{15}N\text{-}NO_3^-$ and $\delta^{18}O\text{-}NO_3^-$ were -10.3±1.7 and 10.1±1.5,
203 respectively for nitrate from nitrification (Mayer et al., 2001), 0±3 and 22±3, respectively
204 for NO_3^- fertilizer (Mayer et al., 2002), and 3±3 and 69±5, respectively for atmospheric
205 nitrate (Burns and Kendall, 2002; Divers et al., 2014). The wastewater $\delta^{15}N\text{-}NO_3^-$ and

206 $\delta^{18}O\text{-}NO_3^-$ end-member values (31.5±7.8 and 11±4.5, respectively) were based on
207 averaging the effluent nitrate isotope values measured monthly from Blue Plains during
208 the study period. The nitrification source represents NO_3^- from nitrification in the water
209 as well as nitrification of ammonia fertilizer in the watershed. The fertilizer source
210 represents synthetically produced NO_3^- fertilizer, not the more common ammonia
211 fertilizer. Animal manure was not used as one of the end-members because this source is
212 more significant in the upper Potomac River, above Washington, D.C. compared to the
213 Lower Potomac River watershed. For example, there are 171 concentrated animal
214 feeding operation (CAFOs) in Upper Potomac compared to 25 CAFOs in the lower
215 Potomac below DC (U.S. EPA, 2016).
216 Due to the variability in nitrate source endmembers, the mixing model was used
217 primarily for illustrative purposes and should be viewed with caution (particularly with
218 regard to identifying other sources besides wastewater). For example, there can be high
219 variability in the nitrification source endmembers because nitrate from nitrification can
220 come from ammonia fertilizer, manure fertilizer, particulate organic matter within the
221 water column, etc. The nitrate from nitrification will therefor carry a range of nitrate
222 isotope values reflecting its original source (Kendall et al., 2007). Also, because
223 denitrification is known to cause the increase in $\delta^{15}N\text{-}NO_3^-$ and $\delta^{18}O\text{-}NO_3^-$ values through
224 isotopic fractionation in approximately a 2:1 relationship (Divers et al., 2014; Kendall et
225 al., 2007), this isotopic enrichment can complicate the identification of wastewater
226 nitrate. As a result, water samples with increased wastewater nitrate, based on the mixing
227 model, may also indicate denitrification has played a role in the isotopic levels of the
228 sample nitrate.

2.6 Salinity *vs*. Nitrate Concentrations and Isotope Mixing Plots

An additional method using plots of salinity *vs.* NO_3^- concentration or NO_3^- isotopes was used to assess whether there is conservative mixing (dilution), or mixing with additional NO_3^- sources down-estuary, or losses of NO_3^- through biotic uptake or denitrification (Middelburg and Nieuwenhuize, 2001; Wankel et al., 2006). Mixing line equations for NO_3^- concentrations were based on equations 1-3 from Middelburg and Nieuwenhuize (2001) and isotopes mixing lines were based on equation 4 from Middelburg and Nieuwenhuize (2001). The mixing line equations and endmember values used for salinity and nitrate isotopes are provided in supporting information (Table S2). Based on those equations, the salinity *vs*. NO_3^- concentration mixing lines are linear, while the mixing lines for NO_3^- isotopes are non-linear (Middelburg and Nieuwenhuize, 2001). Wankel et al. (2006) suggests that when nutrient concentrations fall above the mixing line this indicates an additional source to raise the concentrations, while concentrations that fall below the mixing line indicate that there is a nutrient sink (e.g., denitrification, assimilation, etc.). For nitrate isotopes, when the $\delta^{15}N\text{-}NO_3^-$ and $\delta^{18}O\text{-}NO_3^-$ values fall above this mixing line, this could indicate an additional source or the fractionation of nitrate from assimilation or denitrification that would increase the heavy isotope levels, while isotope values below the mixing line could indicate an additional source of nitrate with lighter isotope values, such as from nitrification or fertilizer sources (Wankel et al., 2006).

2.7 Estuarine Net Fluxes of Nitrogen

A box model was used to estimate net fluxes of TN, NO_3^-, and nitrate isotope loads along the Potomac River Estuary using methods modified from Officer (1980), Boynton et al. (1995), Hagy et al. (2000), and Testa et al. (2008), which are widely used methods for tracking nutrient fluxes in estuaries between different salinity zones. First, the Potomac Estuary was divided into 6 boxes in order to accommodate adequate sampling stations per box, and to evaluate net fluxes at key locations along the estuarine gradient (Fig. 2). Next, due to the Potomac Estuary having a semi-diurnal tidal cycle, where there is movement back and forth across boundaries of the box model, mean monthly freshwater discharge inputs to the first box (USGS, 2014) and interpolated salinity values (measured monthly from surface and bottom waters throughout the system) were used to calculate advective and diffusive exchanges of water and salt between adjacent boxes. Salt balances were then used to compute net exchanges at the boundaries of the six model boxes, similar to previous estuarine box model studies (e.g. Boynton et al., 1995; Hagy et al., 2000). Average monthly TN, NO_3^- and NO_3^- isotope concentrations (collected from the surface and bottom water at each station, except for NO_3^- isotopes, which were collected from the surface only) were multiplied by net estimated exchange values at the box boundaries and summed to calculate the N load leaving or entering each box. In order to calculate the loads for NO_3^- isotopes, the $\delta^{15}N$-NO_3^- and $\delta^{18}O$-NO_3^- values in per mil (‰) were converted to concentrations (μg/L) by multiplying the NO_3^- concentration of the sample by R, the ratio of the heavy to light isotope ($^{15}N/^{14}N$ or $^{18}O/^{16}O$). Fluxes were estimated for each month during the sampling period and then averaged to find seasonal estimates of N fluxes for the Potomac. The

box model results were used to compute: (1) the total inputs of N, (2) the % inputs of loads from Blue Plains, (3) the net export of N to the Chesapeake Bay, (4) the % of Blue Plains inputs that are exported, (5) the net loss in loads along the estuary, and (6) the contribution of N loads from the Chesapeake Bay through tidal inflow.

To account for uncertainty in monthly load estimates, error propagation (using standard errors) was used for each of the hydrologic and nutrient inputs to the model. For example, the error in discharge data came from averaging the mean daily discharge for each month, the error in water concentrations came from averaging the surface and bottom water concentrations, and the error in N from atmospheric deposition came from averaging the weakly deposition data for each month. These uncertainties in the inputs to the box model were then propagated for each of the box model calculations, similar to Filoso and Palmer (2011).

Inputs to the box model include, total monthly precipitation data based on averaging data from three stations along the Potomac Estuary (Precipitation data is from the NOAA National Centers for Environmental Information, Climate Data Online), monthly estimates of atmospheric deposition for NH_4^+, NO_3^-, and DIN (obtained from the National Atmospheric Deposition Program / National Trends Network), NO_3^- concentrations and isotope levels in atmospheric deposition (from Buda and DeWalle, 2009, for the nearby central Pennsylvania region for the year 2005, which was a similar year hydrologically (as described below)), freshwater and N inputs from the land (from Chesapeake Bay model output from 2005), surface and bottom water nutrient and salinity concentrations (from MD DNR), and inputs from the Blue Plains wastewater treatment plant. Also, while there are no USGS gages located along the Potomac Estuary, there is

298 one USGS gage (USGS 01646580) located directly above the Estuary, above the fall line
299 (the location where the hydryodynamics of the river cease being tidally influenced) and
300 this gage was used to account for freshwater inputs into the first box. The model also
301 takes into account water temperature and evaporation.

302 In the box model we made two assumptions regarding the 14 other WWTPs that
303 are dispersed along the estuary below Blue Plains. All, but one of these WWTPs has
304 tertiary treatment (the other has secondary treatment) (www.epa.gov/npdes). These other
305 WWTPs have a combined TN load that is 32% of the TN load from Blue Plains. While
306 the loads from these WWTPs are indirectly accounted for in the box model due to their
307 impact on the concentrations in the estuarine water, it was not feasible to directly
308 incorporate the loads from each WWTP into the box model estimates and thus there may
309 be some added uncertainties. However, we can first assume that the estimated decline in
310 nitrogen loads from the Blue Plains wastewater treatment plant to the mouth of the
311 Potomac River Estuary result in conservative estimates. The additional load from the
312 other WWTPs only adds to the loads estimated further down estuary and consequently
313 the measured loss in N load from the Blue Plains wastewater load down-estuary (the
314 difference between the loads at the mouth and at the head of the estuary) is a conservative
315 estimate because it is less then would be expected, underestimating biological
316 assimilation and removal. Second, for modeling purposes, we also assume here that the
317 loads from the 14 other WWTPs have little effect on the nitrate isotope signal. While
318 $\delta^{15}N\text{-}NO_3^-$ and $\delta^{18}O\text{-}NO_3^-$ isotope values were not measured directly for the 14 other
319 down-estuary wastewater treatment plants, based on the literature, the values for average
320 WWTP nitrate isotopes are typically lower (~10‰ for $\delta^{15}N\text{-}NO_3^-$ and ~0 for $\delta^{18}O\text{-}NO_3^-$)

compared to 31.5‰ for $\delta^{15}N\text{-}NO_3^-$ and 11‰ $\delta^{18}O\text{-}NO_3^-$ for Blue Plains (Kendall et al., 2007; Wang et al., 2013; Wankel et al., 2006). As a result, we expected the other WWTPs to have a similar or an even less pronounced wastewater isotope signal compared to Blue Plains, which has biological nitrogen removal (i.e. denitrification is promoted within the Blue Plains WWTP), elevating the $\delta^{15}N\text{-}NO_3^-$ and $\delta^{18}O\text{-}NO_3^-$ isotope values at Blue Plains more (Kendall et al., 2007). Consequently, the estimated nitrate loads down-estuary incorporate Blue Plains and nitrate inputs from the other WWTPs. They are considered conservative estimates because the additional WWTPs only add to the TN loads and wastewater NO_3^- isotope signal, so any decline in an isotope signal that we attribute to Blue Plains would likely be greater if data availability permitted us to specifically parameterize the isotope values for additional WWTP inputs.

Another assumption was made for the box model related to estuarine mixing. Although portions of the lower estuary can be seasonally stratified, we assumed each box to be well mixed vertically as no bottom water isotope values were available to constrain a 2-layer box model. This assumption is supported by other bottom water data that is available and by samples taken along the width of the estuary. For example, we have conducted the box model and other analyses with and without bottom water isotope data and found minimal change in results (Fig. S1). Our measurements of various biogeochemical signatures at the station close to the estuarine turbidity maximum suggests that there is intense mixing at this site, and prior studies have documented extensive mixing in the freshwater tidal portion of the system (Elliott, 1976, 1978; Pritchard, 1956). Also, it can be assumed that because wastewater effluent inputs are freshwater, much of the effluent plume would likely not sink in the more dense estuarine

344 waters moving up from the bay. Additionally, our box model estimates of net fluxes was
345 compared to a complex, 3 dimensional hydrodynamic model (described below) that
346 incorporates stratification, and this comparison provided support for the low impact of
347 assuming mixing in our approach.

348 Only surface water samples were analyzed for $\delta^{15}N\text{-}NO_3^-$ and $\delta^{18}O\text{-}NO_3^-$ isotopes,
349 and as a result our box model was not able to directly incorporate the potential impacts of
350 stratification on the estimated flux of NO_3^- isotopes. However, while seasonal
351 stratification has been found close to the mouth of the of the Potomac estuary (Hamdan
352 and Jonas, 2006), using documented nitrate bottom water isotope values from near the
353 mouth of the estuary (Horrigan et al., 1990) we calculate that incorporating bottom water
354 isotope values would have a minimal impact on the flux estimates of our box model,
355 particularly when not including spring 2011 (Fig. S1). But when including spring 2011,
356 and using the reported values of 10‰ for bottom water $\delta^{15}N\text{-}NO_3^-$, based on Horrigan et
357 al. (1990), in Boxes 5 and 6 where stratification is most likely, our estimates for the flux
358 of $\delta^{15}N\text{-}NO_3^-$ from these boxes increases by 20% on average, and the net loss in load
359 from box 1 to box 6 increases by 12% on average. This indicates that our estimates are
360 conservative because by not using bottom water we estimate a smaller net loss in $\delta^{15}N\text{-}$
361 NO_3^- (Fig. S1).

362 For the box model we also assumed the estuary to be well mixed laterally. In
363 terms of potential variability for samples taken at different locations along the width of
364 the estuary, there was found for surface water samples, on average, a 6±3% difference in
365 $\delta^{15}N\text{-}NO_3^-$, a 7±3% difference in $\delta^{18}O\text{-}NO_3^-$, a 24±8% difference in NO_3^-, and a 15±3%
366 difference in TN (based on samplings that were done at two or more locations along the

same longitudinal transect at approximately the same distance down-estuary, but at different locations horizontally at that location). Based on this, the nitrate isotopes values and NO_3^- and TN concentrations appear to show that the estuary is fairly well mixed laterally.

To assess the accuracy of the box model assumptions and results, estimated net fluxes of total N were compared to simulation output from the Chesapeake Bay Water Quality Model. This model was developed by the U.S. EPA to aid in efforts to set TMDLs for the Chesapeake Bay (Cerco et al., 2010), and combines a 3-D hydrodynamic model (CH3D) with a water quality model (CE-QUAL-ICM). Simulation output data were available for 1996, 2002, and 2005. We selected a simulation year (2005) because it had similar river discharge conditions to 2010, and compared modeled net fluxes of TN at three boundary locations to estimates at the same (or nearby) box model boundaries.

2.8 Statistical Analyses

Statistical analyses were performed using the statistical package R (R Development Core Team, 2013). Linear regression was used to test for significant changes in stream chemistry and nitrate isotope data with distance down estuary. Repeated measures analysis of variance (ANOVA) was used to test for seasonal differences in nitrate isotopes trends with distance.

3 Results

3.1 Spatial and Temporal Trends in N Concentrations

Longitudinal patterns of dissolved inorganic nitrogen (DIN) in the lower Potomac River showed an increase in concentrations near and directly below the Blue Plains wastewater treatment plant and then a steady decline in concentrations down to the Chesapeake Bay (Fig. 3a). The implementation of tertiary treatment in 2000 coincided with a significant drop in annual average DIN concentration directly down-estuary of the Blue Plains WWTP (from 1.7 ± 0.02 to 1.3 ± 0.01 mg/l, $p < 0.05$) (Fig. 3a), when comparing years directly prior (1997-1999) and the years directly after 2000 (2001-2005). However, the impact of the wastewater treatment plant improvements on reducing longitudinal patterns of DIN was only apparent for the first 30 km down-estuary. After this, both the pre- and post-2000 DIN concentrations overlapped (Fig. 3a). As DIN decreased longitudinally down-estuary of the wastewater treatment plant, there was also a small, but significant increase in total organic nitrogen (TON) after the year 2000 ($p < 0.01$, Fig. 3a), not including the last sample near the mouth of the estuary, which is likely influenced by tidal inflow.

There were seasonal variations in DIN concentrations along the Potomac River Estuary with the greatest concentrations in the winter and spring (Fig. 3b). There is also a steeper decline in DIN with distance during fall, winter, and summer compared to the spring ($p < 0.05$, Fig. 3b). The average molar ratio of DIN to PO_4^{-3} (N:P ratio) showed an initial increase, then a decrease as estuarine salinity started to increase (Fig. 3c). During the summer and fall, the N:P ratio fell below the Redfield ratio (16:1, the atomic ratio of nitrogen and phosphorus found in oceans and phytoplankton), around 40 km

409 down-estuary and stayed below 16, which indicated a shift from P to N limitation.
410 During the winter and spring, the N:P ratio never fell below 16 and increased steadily
411 after 50 km down-estuary (Fig. 3c). There was also a significant negative relationship
412 between NO_3^- and DOC concentration during the study period ($p < 0.01$, Fig. 4).
413
414 **3.2 Spatial and Seasonal Trends in NO_3^- Isotopes and Sources**
415 During each season, except spring, $\delta^{15}N\text{-}NO_3^-$ values increased sharply at the
416 Blue Plains outfall, from 9.3 ± 1.4 ‰ up-estuary to 25.7 ± 2.9 ‰ at the outfall ($p < 0.05$),
417 and then rapidly decreased within 2 km down-estuary of the Blue Plains WWTP to 15.7 ±
418 2.2 ‰ ($p < 0.05$, Fig. 5a). During the summer and fall, the $\delta^{15}N\text{-}NO_3^-$ values showed the
419 largest increase near the effluent outfall (except for one very high winter value) and then
420 a significant decrease ($p < 0.05$) with distance down-estuary. There was also a slight
421 increase in $\delta^{15}N\text{-}NO_3^-$ and $\delta^{18}O\text{-}NO_3^-$ values from 1 to 6 km down-estuary (Fig. 5a,b).
422 During the winter and spring, the $\delta^{15}N\text{-}NO_3^-$ and $\delta^{18}O\text{-}NO_3^-$ values remained relatively
423 constant throughout the estuary, even near Blue Plains (Fig. 5a,b), while during the
424 summer and fall the $\delta^{15}N\text{-}NO_3^-$ and $\delta^{18}O\text{-}NO_3^-$ values steadily declined after 6-10 km
425 down-estuary (Fig. 5a,b). At the mouth of the estuary, the $\delta^{15}N\text{-}NO_3^-$ values for all
426 seasons were roughly equivalent (Fig. 5a). During the summer and fall, the $\delta^{18}O\text{-}NO_3^-$
427 values showed a steady decrease after 12 km down-estuary, while they increased during
428 spring and winter (Fig. 5b).
429 Based on the nitrate isotope mixing model, nitrate contributions from wastewater
430 ranged from 80 ± 13% at the wastewater outfall to 57 ± 11% within the first 1 km down-
431 estuary. Wastewater nitrate contributions then decreased to 44 ± 14% at the confluence

of the Potomac River Estuary with Chesapeake Bay (Fig. 5c), suggesting that there was a $36 \pm 19\%$ loss in wastewater NO_3^- along the estuary annually. Nitrate from nitrification (of N from upriver manure or ammonia fertilizer and also Blue Plains wastewater N) increased from $13 \pm 12\%$ at the wastewater outfall to $29 \pm 22\%$ at the confluence of the Potomac River Estuary with Chesapeake Bay (Fig. 5c). Nitrate from fertilizer increased from $6 \pm 6\%$ at the wastewater outfall to $22 \pm 22\%$ at the confluence of the Potomac River Estuary with Chesapeake Bay (Fig. 5c). Nitrate from atmospheric deposition changed little along the Potomac Estuary from 1 ± 1 at the wastewater outfall to 5 ± 5 at the confluence with the Chesapeake Bay (Fig. 5c). At the last two sampling stations near the mouth of the Potomac River Estuary, NO_3^- from fertilizer showed an increase, while NO_3^- from nitrification showed a corresponding decline (Fig. 5c).

3.3 $\delta^{15}N\text{-}NO_3^-$ and $\delta^{18}O\text{-}NO_3^-$, NO_3^- Concentration, and Salinity Relationships

The Blue Plains effluent and Potomac River samples within 20 km downriver of the wastewater treatment plant showed a significant positive relationship between $\delta^{15}N\text{-}NO_3^-$ and $\delta^{18}O\text{-}NO_3^-$ ($p < 0.05$) (Fig. 6a). When denitrification and biotic uptake occurs, plotting $\delta^{15}N\text{-}NO_3^-$ *vs.* $\delta^{18}O\text{-}NO_3^-$ shows a 2:1 relationship (Kendall et al. 2007). The Blue Plains effluent samples showed approximately a 2.4 to 1 relationship. The samples within 20 km downriver showed a 3:1 ratio (Fig. 6a). The nitrate samples within the first 6 km showed a 2.4 to 1 relationship (Fig. 6a). There were also seasonal differences in the relationship between $\delta^{15}N\text{-}NO_3^-$ and $\delta^{18}O\text{-}NO_3^-$ (Fig. 6b); spring, summer, and fall were characterized by close to a 2:1 relationship between $\delta^{15}N\text{-}NO_3^-$ *vs.* $\delta^{18}O\text{-}NO_3^-$, while winter showed a ~8:1 relationship.

Because salinity is a conservative tracer, plots of salinity *vs.* NO_3^-, $\delta^{15}N\text{-}NO_3^-$, and $\delta^{18}O\text{-}NO_3^-$ can indicate effects of mixing between water at the tidal freshwater section with water from the mesohaline section of the Potomac River Estuary. Deviations from the mixing lines can indicate additional sources or biological transformations (Middelburg and Nieuwenhuize, 2000; Wankel et al., 2006). Surface water NO_3^- concentrations and nitrate isotopes fell on (for $\delta^{18}O\text{-}NO_3^-$) or slightly below mixing line (for $\delta^{15}N\text{-}NO_3^-$) during the spring (Fig. 7a,b,c), which indicated mostly conservative mixing (dilution or inputs from low $\delta^{15}N\text{-}NO_3^-$ like nitrification). But during the summer and fall, the NO_3^- concentration and isotope values fell well below the mixing lines. During the winter, the values fell both above and below the mixing line (Fig. 7a,b,c), which indicated non-conservative mixing.

3.4 Spatial and Seasonal Trends in N Loads

Our comparisons of box model net exchange estimates with simulation output provided by the Chesapeake Bay Program Eutrophication Model ("Bay Model") revealed similar TN loads between our results and the Bay Model in the winter, spring, and fall, with the largest differences in the models evident in the summer months at the boundary location where tidal fresh transitions to oligohaline conditions and at the mouth of the estuary (Table S3 and Figures 8 and 9). Even so, these differences are smaller than a factor of 2 for winter and spring and for most of the summer and fall. Despite the assumption of complete mixing in our box model, this is a good agreement considering the simplification of hydrodynamics inherent to a box modeling approach when compared to the highly constrained CH3D hydrodynamic modeling platform (Cerco et

al., 2010). The Potomac estuary is well mixed along two thirds of its length, and this likely contributes to our success in applying a single layer box model to this system. The box model also permitted estimates of TN loads at smaller spatial scales than the three boundaries available from the Chesapeake Bay Program, which could enable a better interpretation of where Blue Plains effluent was subject to transformations in the oligohaline portion of the estuary (Fig. 8). The caveat here is that box-modeled summer loads should be interpreted with caution because they show the greatest differences from the CH3D model.

Results of the box model indicate that an annual average of $8.4 \times 10^6 \pm 4.8 \times 10^6$ kg/yr of TN are exported to the Bay and the net loss in load for TN along the estuary (from Blue Plains to the mouth of the estuary), attributed to assimilation, burial and denitrification, was $9.1 \times 10^6 \pm 5.1 \times 10^6$ kg/yr of TN. Using an N burial rate of $2.49 \times 10^6 \pm 3.1 \times 10^5$ kg/yr (Harris, unpublished data), a denitrification rate of $6.17 \times 10^6 \pm 8.3 \times 10^4$ kg/yr (Cornwell et al., 2016) and a fisheries yield rate of 0.82×10^6 kg/yr (Boynton et al., 1995) , we see that our box model estimate is nearly balanced by independently estimated values for these loss terms. On a mean annual basis, denitrification accounts for about 68 ± 1% of the loss in TN, burial is estimated to account for 27 ± 3%.2 of the loss in TN, and assimilation into fisheries accounts for approximately 9% of loss in TN load along the Potomac Estuary.

The net load (kg/day) of TN, NO_3^-, and $\delta^{15}N\text{-}NO_3^-$ decreased down-estuary during each season (Fig. 10a-c, $p < 0.05$ for winter and spring and $p < 0.1$ for summer and fall). N loads were highest along the estuary during spring and winter (Fig. 10), and there was a greater decline in TN loads on average from box 1 to box 6 during winter and spring (a

501 loss of ~27,000 ± 15,000 and 50,000 ± 52,000 kg/day, respectively) (Table 1) compared
502 to summer and fall (a loss of ~7,000 ± 8,000 and 15,000 ± 13,000 kg/day, respectively).
503 However, the summer and fall months showed a greater percent decline in TN (75 ± 75%
504 and 112 ± 95%, respectively) compared to winter and spring (54 ± 40 and 36 ± 43%,
505 respectively). The relatively high errors are primarily from the larger uncertainty found
506 in the last box, at the mouth of the estuary, due to the larger size of this box and greater
507 uncertainty in fluxes at the mouth of the estuary; the uncertainties are much smaller
508 further up-estuary (See Fig. 10a). NO_3^- and $\delta^{15}N\text{-}NO_3^-$ follow the same seasonal patterns
509 as TN. Also, winter, along with summer and fall, showed a greater percent decline in
510 NO_3^- and NO_3^- isotope loads compared to spring (Table 1).
511 The percent contribution of TN inputs from the Blue Plains wastewater treatment
512 to the main stem of the Chesapeake Bay ranged from 8 to 47 % (Table 1). The
513 contribution was significantly lower during the winter and spring (10 ± 13 and 8 ± 1%,
514 respectively) compared to summer and fall (38 ± 3 and 47 ± 13%, respectively, Table 1),
515 when TN fluxes from all sources are relatively low. The percent of Blue Plains
516 wastewater TN inputs that are exported to the Chesapeake Bay ranged from <4 to 71%,
517 and they were highest in the spring (71 ± 20%, Table 1). There were also N inputs to the
518 Potomac river-estuarine continuum from the Chesapeake Bay during each season, except
519 spring, due to higher flows (Table 1 & 2) because flow in spring was too high to allow
520 the inputs from the Bay that occurred in the other seasons. NO_3^- and $\delta^{15}N\text{-}NO_3^-$ follow
521 the same seasonal patterns as TN, showing the greatest percentage of inputs from Blue
522 Plains exported during the spring.
523

4 Discussion

While coastal urbanization can have a major impact on water quality in receiving waters, the results of this study suggest that rivers and estuaries also show a large capacity to transform and bury anthropogenic N. In particular, our results indicate that up to 95% of inputs of N from the Washington D.C. Blue Plains wastewater treatment plant were removed *via* burial or denitrification along the Potomac river-estuarine continuum, depending on the season (Table 1). Recent work shows that urban watersheds and river networks can also be "transformers" of nitrogen across similar broad spatial scales, which impacts downstream coastal water quality (Kaushal et al., 2014a). Here, we show that the urban river-estuarine continuum also acts as a transformer and can have large impacts on the sources, amounts, and forms of nitrogen transported to the Chesapeake Bay. Our results showed that N transformation varied across seasons and hydrologic conditions with important implications for anticipating changes in sources and transport of coastal nitrogen pollution in response to future climate change. This is particularly significant, given long-term increases in water temperatures of major rivers and increased frequency and magnitude of droughts and floods in this region and elsewhere (e.g. Kaushal et al., 2010a; Kaushal et al., 2014b).

4.1 Spatial and Temporal Trends in N Concentrations and Loads

The decrease in DIN concentrations with distance down-estuary is largely from denitrification, assimilation, and burial, as indicated by the inverse relationship between NO_3^- concentrations and DOC and TON concentrations, the NO_3^- isotope data, and N mass balance data. Dilution from tidal marine waters plays a minor role in the decrease

547 in DIN and the incoming tidal waters may even contribute to DIN as suggested by the
548 decrease in DIN slope after 130 km down estuary (Boynton et al., 1995), depending on
549 the season. The installation of tertiary wastewater treatment technology at Blue Plains in
550 the year 2000 showed a significant drop in DIN concentrations within 20-30 km of Blue
551 Plains. However, the DIN concentrations below 30 km down-estuary were
552 approximately the same based on an annual average, before and after the year 2000. One
553 explanation is that the dissolved wastewater N is completely assimilated into particulate
554 organic matter (supported by the inverse NO_3^- *vs.* TON or DOC relationships (Fig.s 3a
555 and 4) or removed by denitrification (as suggested by the isotope data) within the first 10
556 km down-estuary, and thus the majority of DIN below 30 km is from other inputs than
557 the Blue Plains wastewater treatment plant. For example, there are 14 other smaller
558 wastewater treatment plants along the Potomac River Estuary, which contribute a total of
559 about 270 mgd (almost as much as the amount Blue Plains contributes) and they could
560 offset further decreases in NO_3^- concentrations down-estuary. Also, our isotope mixing
561 model data shows that nitrification (likely of upriver manure or ammonia fertilizer
562 inputs) and fertilizer are important sources further down-estuary; and 42% of the land-use
563 along the Potomac Estuary is agriculture (Karrh et al., 2007b). A second explanation
564 could be related to a change in N:P ratio with distance down-estuary. Specifically, there
565 was a rise in estuarine salinity around 30 to 50 km down-estuary and a coinciding
566 increase in dissolved PO_4^{-3} concentration (typical of the estuarine salinity gradient)
567 (Jordan et al., 2008). When the N:P ratio fell below the Redfield Ratio of 16:1, the
568 estuary could shift from P limitation to N limitation (Fisher et al., 1999). The potential
569 shift from P to N limitation occurred 40-50 km down-estuary, around the estuarine

570 turbidity maximum, which is associated with higher estuarine bacterial productivity
571 (Crump and Baross, 1996), and may be driving DIN removal further down-estuary.
572 Mass balance indicates that TN and NO_3^- loads decreased down-estuary each
573 season (despite inputs from the 14 other wastewater treatment plants down-estuary). The
574 $8.4 \times 10^6 \pm 4.8 \times 10^6$ kg/year of TN exported to the Bay annually is close to the $14.1 \times$
575 10^6 kg/yr estimated by Boynton et al. (1995). The net loss in load for TN along the
576 estuary ($9.1 \times 10^6 \pm 5.1 \times 10^6$ kg/yr), attributed to burial and denitrification was also
577 similar to the sum of the burial and denitrification rates estimated by Boynton et al.
578 (1995) for the lower Potomac (13.3×10^6 kg/year of TN). Also, our comparison of net
579 losses in TN along the estuary with independent estimates of burial (Harris, unpublished
580 data), denitrification rate (Cornwell et al., 2016), and assimilation (Boynton et al., 1995)
581 also closely align with our estimate for the net loss in load for TN along the estuary. .
582 The large loss in TN load attributed to denitrification ($68 \pm 1\%$) is supported by the NO_3^-
583 isotope data indicating that there was likely denitrification (and assimilation) of NO_3^-,
584 particularly within 6 km down-estuary from the Blue Plains wastewater treatment plant.
585 Over seasonal time scales, there was a greater percent decline in TN loading during
586 summer and fall, likely due to warmer temperatures and increased biological
587 transformation (attributable to high rates of phytoplankton uptake and detrital deposition)
588 (Eyre and Ferguson, 2005; Gillooly et al., 2001; Harris and Brush, 2012; Nowicki, 1994),
589 which suggested that the urban river-estuarine continuum may be more efficient at
590 removing TN during the summer and fall. Compared to summer and fall, winter also had
591 a relatively high percent decline in NO_3^- loads possibly driven by the higher
592 concentrations typically found in winter months, which could result in quicker

593 assimilation through first order reaction rate kinetics (Betlach and Tiedje, 1981). Since
594 there was no evidence for denitrification during the winter, burial could also be a
595 mechanism for the relative high decline in winter months, which is typical of higher
596 flows (Boynton et al., 1995; Milliman et al., 1985; Sanford et al., 2001). However, more
597 work is necessary to evaluate the fate of nitrate using ecosystem process level
598 measurements.

599 The higher total exports of TN and NO_3^- to Chesapeake Bay during the winter and
600 spring are due to greater N inputs from the upper and lower watershed and/or greater
601 flow rates. The proportion of N exports attributed to Blue Plains wastewater treatment
602 plant were the highest in the spring, likely due to shorter water residence times (Table 2),
603 resulting in less time for biological uptake, removal, or burial of N. The greater decline
604 in N loads during the spring, however, may be attributed to multiple factors, such as
605 greater N loads being imported from the upper estuary and higher concentrations,
606 compared to summer and fall (Table 1) and thus driving greater losses (from burial and
607 denitrification) due to first order reaction rate kinetics (Betlach and Tiedje, 1981) similar
608 to winter (described above), stratification that is characteristic of higher flows (Boesch et
609 al., 2001), and increased burial rates due to greater sediment loads during higher flows
610 (Milliman et al., 1985; Sanford et al., 2001). As mentioned previously, more work is
611 necessary regarding linking ecosystem processes and microbial dynamics with the fate of
612 nitrate in the estuary. Nonetheless, the decline in TN and NO_3^- loads down-estuary each
613 season provide strong evidence for the transformation and retention of N along estuaries.
614

4.2 Spatial Trends in NO_3^- Sources and Role of Denitrification, Assimilation and Nitrification

The Potomac River estuary was a transformer of wastewater N inputs from the Washington D.C. metropolitan area to its confluence with Chesapeake Bay. The values for $\delta^{15}N\text{-}NO_3^-$ above the wastewater treatment plant were relatively high, suggesting upriver sources may primarily be from animal waste (Burns et al., 2009; Kaushal et al., 2011; Kendall et al., 2007). This is consistent with a previous study, which found that 43% of N inputs to the upper Potomac River are from manure (Jaworski et al., 1992), while the lower Potomac River has more fertilizer and combined animal feeding operations (CAFOs) (U.S. EPA, 2016). Effluent inputs from the Blue Plains wastewater treatment plant significantly increased the $\delta^{15}N\text{-}NO_3^-$ values even further, yet this NO_3^- signal from wastewater disappeared after 20-30 km down-estuary. The increase in $\delta^{15}N\text{-}NO_3^-$ and $\delta^{18}O\text{-}NO_3^-$ values within the first 1 to 6 km down-estuary suggest denitrification or assimilation of nitrate, due to the lighter $\delta^{14}N\text{-}NO_3^-$ and $\delta^{16}O\text{-}NO_3^-$ isotopes being preferentially denitrified or assimilated and leaving behind the heavier nitrate isotopes (Granger et al., 2008; Granger et al., 2004; Kendall et al., 2007). But the gradual decline in both $\delta^{15}N\text{-}NO_3^-$ and $\delta^{18}O\text{-}NO_3^-$ values from 6 km to 160 km down-estuary indicates nitrification dominates this portion of the estuary (supported by the nitrate isotope mixing model results) because the process of nitrification, which converts ammonia to nitrate results in lighter nitrate isotopes being generated through fractionation (Kendall et al., 2007; Vavilin, 2014). However, the decline in $\delta^{15}N\text{-}NO_3^-$ and $\delta^{18}O\text{-}NO_3^-$ loads corresponding with the decline in overall NO_3^- loads down-estuary also suggests that the heavy nitrate isotopes are being removed as well as the light isotopes. The

disappearance of $\delta^{15}N\text{-}NO_3^-$ and $\delta^{18}O\text{-}NO_3^-$ down-estuary where NO_3^- concentrations are very low (~0.01 mg/l) may indicate that assimilation or even denitrification is occurring on the remaining heavy $\delta^{15}N\text{-}NO_3^-$ or $\delta^{18}O\text{-}NO_3^-$ after the lighter $\delta^{14}N\text{-}NO_3^-$ or $\delta^{16}O\text{-}NO_3^-$ is all used up (Fogel and Cifuentes, 1993; Vavilin et al., 2014; Waser et al., 1998a; Waser et al., 1998b).

Seasonal differences in the longitudinal trends for $\delta^{15}N\text{-}NO_3^-$ and $\delta^{18}O\text{-}NO_3^-$ suggest differences in biological transformations of nitrate due to differences in water temperature, hydrology, and/or N inputs. The $\delta^{15}N\text{-}NO_3^-$ values from effluent inputs were higher in warmer months due likely to higher denitrification rates in the wastewater treatment plant associated with warmer water temperatures (Dawson and Murphy, 1972; Pfenning and McMahon, 1997), resulting in elevated $\delta^{15}N\text{-}NO_3^-$ values produced by isotopic fractionation (Kendall et al., 2007; Mariotti et al., 1981). An increase in $\delta^{15}N\text{-}NO_3^-$ between 2 and 6 km down-estuary during summer and fall (Fig. 5b) further shows increased denitrification or biological uptake due to warmer water temperatures and fractionation (Eyre and Ferguson, 2005; Gillooly et al., 2001; Harris and Brush, 2012; Nowicki, 1994). The significant drop in $\delta^{15}N\text{-}NO_3^-$ beyond 10 km down-estuary during summer and fall may have been due to mixing with other N sources and increased nitrification (Wankel et al., 2006), indicated by the salinity mixing line results. During the spring, there was also a significant decline in $\delta^{15}N\text{-}NO_3^-$ between 10 and 160 km down-estuary, but this was likely attributed to dilution and nitrification, based on the conservative mixing results. The lack of a significant change during the winter, may be due to shorter residence times (Table 2) and cooler temperatures, contributing to lower biological transformation rates. Further down-estuary, near the mouth of the estuary, the

661 increase in $\delta^{18}O\text{-}NO_3^-$ in winter and spring might indicate denitrification in the estuary
662 but in spring nitrate seems conservative based on the salinity mixing plots. The decline in
663 $\delta^{18}O\text{-}NO_3^-$ down-estuary in summer and fall suggest that processes other than
664 denitrification in the estuary are controlling the $\delta^{18}O\text{-}NO_3^-$, such as nitrification.
665
666 **4.3 Isotope and Salinity Mixing Models and Influence of Temperature and**
667 **Residence Time**
668 Seasonally, the ~2:1 relationship between $\delta^{15}N\text{-}NO_3^-$ and $\delta^{18}O\text{-}NO_3^-$ during
669 spring, summer and fall, may indicate denitrification or assimilation, but the salinity
670 mixing plots suggests no denitrification in the spring. The fact that the $\delta^{15}N$:$\delta^{18}O$ ratio is
671 between 1 and 2 for summer and fall may mean assimilation plays a role, which is
672 supported by previous studies that found a 1:1 relationship for assimilation in the marine
673 environment (Granger et al., 2004; Karsh et al., 2012; Karsh et al., 2014). However,
674 other previous studies suggest that a $\delta^{15}N$:$\delta^{18}O$ ratio between 1 and 2 can also be caused
675 by denitrifying bacteria (Granger et al., 2008; Lehmann et al., 2003). The divergence
676 from 2:1 ratio may also be attributed to hotspots of denitrification, such as in hyporheic
677 zones where nitrate is completely consumed by denitrification, resulting in no
678 fractionation (Fogel and Cifuentes, 1993; Vavilin et al., 2014; Waser et al., 1998a; Waser
679 et al., 1998b). Additionally, the divergence from the 2:1 ratio in samples further down-
680 estuary may indicate mixing between two or more NO_3^- sources, such as between
681 atmospheric, marine, or nitrification (Kaushal et al., 2011; Wankel et al., 2006). Due to
682 water column dissolved oxygen levels averaging over 4 mg/L (data from Chesapeake Bay
683 program, not shown), assimilation likely dominates NO_3^- removal in the water column,

684 while denitrification likely dominates nitrate removal from the sediment, which is
685 supported by previous work (Cornwell et al., 2014; Kemp et al., 1990).
686 Based on the nitrate isotope mixing model, the longitudinal trends in nitrate
687 sources along the Potomac Estuary correspond with the other results of this study. The
688 decline in wastewater nitrate matched the decline in nitrate concentrations and loads,
689 while the slight increases in nitrification and fertilizer both correspond with decline N
690 and O isotopes values down-estuary and the increase agricultural land use in the lower
691 Potomac watershed. Future research would benefit from doing the mixing model
692 separately using different endmembers for the different seasons in order to better
693 constrain the differences between seasons. But due to lack of data on the seasonality of
694 fertilizer and nitrification endmembers it was not feasible for the scope of this paper.
695 Seasonal endmembers could provide more confidence because we found that seasonality
696 and temperature mattered in the N sources and loads. Many isotopic studies do not
697 always take this into account and typically just use literature values; our work showed
698 that there are important seasonal variations and in order to improve the isotope mixing
699 model to capture difference between seasons, the seasonal changes in the endmembers
700 may need to be captured.
701 Denitrification is likely a sink for NO_3^- during the summer and fall based on the
702 increases in $\delta^{15}N\text{-}NO_3^-$ and $\delta^{18}O\text{-}NO_3^-$ within 6 km down-estuary and due to warmer
703 water temperatures, while there is no evidence for denitrification in the winter due to
704 reduced biological activities typical in cooler winter temperatures (Eyre and Ferguson,
705 2005; Gillooly et al., 2001; Harris and Brush, 2012; Nowicki, 1994). Nevertheless,

706 nitrate removal was significant in all seasons, including winter proposing other
707 mechanisms, as indicated by the salinity based mixing lines.
708 Plots of salinity *vs.* NO_3^-, $\delta^{15}N\text{-}NO_3^-$, and $\delta^{18}O\text{-}NO_3^-$ were used to provide
709 evidence for conservative mixing, uptake, production, or contributions from other NO_3^-
710 sources. NO_3^- concentrations fell below the mixing lines during the summer, fall, and
711 winter, suggesting non-conservative mixing behavior due to the presence of a NO_3^- sink,
712 such as assimilation or denitrification (Wankel et al., 2006). During the spring NO_3^-
713 concentrations fell on the mixing line, however, indicating that there were no important
714 sources or sinks. This may be due to higher flows and shorter residence times in the
715 spring (Table 2), which can result in less biological transformations of NO_3^-. In the
716 salinity *vs*. $\delta^{15}N\text{-}NO_3^-$ and $\delta^{18}O\text{-}NO_3^-$ plots, when the isotope values fell below the
717 mixing lines, this suggested the contribution of NO_3^- from sources with lower $\delta^{15}N\text{-}NO_3^-$
718 and $\delta^{18}O\text{-}NO_3^-$, such as fertilizer inputs or nitrification, which produces nitrate with lower
719 $\delta^{15}N\text{-}NO_3^-$ and $\delta^{18}O\text{-}NO_3^-$ values through fractionation (Kaushal et al., 2011; Kendall et
720 al., 2007). An increase in nitrification down-estuary is likely attributed to the conversion
721 of remineralized N to nitrate or from down-estuary inputs of wastewater ammonia that is
722 converted to nitrate (Middelburg and Nieuwenhuize, 2001). During the spring, $\delta^{18}O\text{-}$
723 NO_3^-, isotope values again fell mostly on the mixing line, which may indicate the
724 Potomac River Estuary is acting more like a transporter instead of a transformer (e.g.
725 Kaushal and Belt, 2012), transporting NO_3^- without there being any significant sinks of
726 NO_3^- or mixing with additional sources, likely due to lower residence times (Table 2) in
727 the spring. However, the fact that during the spring the $\delta^{15}N\text{-}NO_3^-$ values were slightly
728 below the mixing line indicates there may have been an increased amount of nitrate

729 inputs from the watershed through runoff carrying nitrate produced by nitrification.
730 During the winter, $\delta^{15}N\text{-}NO_3^-$ values also fell above the mixing line for some samples,
731 which suggested the contribution of heavy $\delta^{15}N\text{-}NO_3^-$ from an additional down-estuary
732 source (potentially from one of the 14 other wastewater treatment plants in the lower
733 Potomac watershed). This was likely not the case during the summer and fall when other
734 sources and sinks may dominate due to greater biological activities (Eyre and Ferguson,
735 2005; Gillooly et al., 2001; Harris and Brush, 2012; Nowicki, 1994) or during the spring
736 when there is more conservative behavior due to higher flows. . Even though only
737 surface water salinity, nutrient, and isotope values were used in these mixing line plots,
738 when bottom water nutrient and isotope data was averaged with the surface water values,
739 the mixing lines plots and results did not change (data not shown).

740 # 5 Conclusion

741 By coupling isotope tracking techniques and a mass balance over broader spatial
742 and temporal scales, we found that an urban river-estuarine continuum in the Chesapeake
743 Bay, and likely similar estuaries globally can transform anthropogenic inputs of N over
744 relatively short spatial scales. Only a small fraction of N inputs from a major wastewater
745 treatment plant were exported out of the estuary. However, processing of N by estuaries
746 can vary considerably across seasons and hydrologic extremes, with greater exports
747 during periods of higher flows and cooler temperatures, and greater transformations and
748 retention during longer hydrologic residence times and warmer temperatures. In
749 particular, this study supports previous work, showing that non-point sources of N were
750 more dominant during winter and spring when runoff from the watershed and estuarine

flows were higher compared to summer and fall when the point-sources were more dominant, due to lower flows. These differences suggest N processing in urban rivers and estuaries would differ from those in non-urban estuaries. Also, the potential for long-term and widespread increase in water temperatures and frequency and magnitude of droughts and floods through climate change (Kaushal et al., 2010a; Kaushal et al., 2014b; Kaushal et al., 2010b), will likely influence the sources and transformation of nitrogen to the Chesapeake Bay and estuaries globally. Consequently, future efforts to manage nutrient exports along rivers and estuaries would benefit from better understanding the interactive effects of land use and climate variability on the sources, amounts, and transformations of N exported to coastal waters and targeting critical times for more intensive wastewater treatment.

Details on Supporting Information

- Additional site information and details on methods
- Table with site coordinates
- Table with mixing model
- Table comparing between box model (this study) and Chesapeake Bay Model.
- A figure comparing box model results with and without bottom water isotope data

Data Availability

Data used for the research in this paper is available through 4TU.centre at the following DOI and URL: doi:10.4121/uuid:e68c6141-f83e-4375-ac3b-088ddf4eff51

http://doi.org/10.4121/uuid:e68c6141-f83e-4375-ac3b-088ddf4eff51

774

775 **Author contribution**

776 This paper is based on work from Michael Pennino's PhD dissertation. Dr. Michael
777 Pennino collected water samples, conducted data analysis, and wrote the manuscript. Dr.
778 Sujay Kaushal contributed to the study design, and provided helpful feedback on data
779 analysis and manuscript writing. Dr. Sudhir Murthy contributed to study design,
780 provided data, and contributed to manuscript revisions. Joel Blomquist contributed to
781 study design, sample collection, and manuscript revisions. Dr. Jeff Cornwell contributed
782 to manuscript revisions and provided feedback on data analysis. Dr. Lora Harris
783 contributed to study design, helped with manuscript writing, and provided significant
784 contributions to data analysis (particularly for the box model mass balance).

785

786 **Acknowledgements**

787 Contact the corresponding author (michael.pennino@gmail.com) regarding the nitrate
788 isotope data. The historical water quality data used in this study was collected by the
789 Maryland Department of Natural Resources and is available free through the Chesapeake
790 Bay Program's Data Hub website:
791 (www.chesapeakebay.net/data/downloads/cbp_water_quality_database_1984_present).
792 This research was supported by the Washington D.C. Water and Sewer Authority. We
793 would like to thank Sally Bowen and Matt Hall from the Maryland Department of
794 Natural Resources (DNR) for their assistance in collecting monthly water samples along
795 the Potomac Estuary and David Brower at the U.S. Geological Survey for help in
796 collecting monthly river input samples for the Potomac River. We acknowledge the input

797 provided by Lewis Linker and Ping Wang of the US EPA Chesapeake Bay Program's
798 Modeling Team for providing simulated output from the CE QUAL ICEM model at three
799 flux boundaries in the Potomac for comparison with our box model output. Gratitude is
800 extended to Dr. Jeremy Testa for his suggestions regarding the box model effort. Tom
801 Jordan also provided helpful suggestions.
802

References

Aitkenhead-Peterson, J. A., Steele, M. K., Nahar, N., and Santhy, K.: Dissolved organic carbon and nitrogen in urban and rural watersheds of south-central Texas: land use and land management influences, Biogeochemistry, 96, 119-129, 2009.

Betlach, M. R. and Tiedje, J. M.: Kinetic explanation for accumulation of nitrite, nitric-oxide, and nitrous-oxide during bacterial denitrification, Applied and Environmental Microbiology, 42, 1074-1084, 1981.

Boesch, D. F., Brinsfield, R. B., and Magnien, R. E.: Chesapeake Bay eutrophication: Scientific understanding, ecosystem restoration, and challenges for agriculture, J. Environ. Qual., 30, 303-320, 2001.

Boynton, W. R., Garber, J. H., Summers, R., and Kemp, W. M.: Inputs, transformations, and transport of nitrogen and phosphorus in Chesapeake Bay and selected tributaries, Estuaries, 18, 285-314, 1995.

Boynton, W. R., Hagy, J. D., Cornwell, J. C., Kemp, W. M., Greene, S. M., Owens, M. S., Baker, J. E., and Larsen, R. K.: Nutrient budgets and management actions in the Patuxent River estuary, Maryland, Estuaries and Coasts, 31, 623-651, 2008.

Buda, A. R. and DeWalle, D. R.: Dynamics of stream nitrate sources and flow pathways during stormflows on urban, forest and agricultural watersheds in central Pennsylvania, USA, Hydrological Processes, 23, 3292-3305, 2009.

Burns, D. A., Boyer, E. W., Elliott, E. M., and Kendall, C.: Sources and Transformations of Nitrate from Streams Draining Varying Land Uses: Evidence from Dual Isotope Analysis, J. Environ. Qual., 38, 1149-1159, 2009.

825 Burns, D. A. and Kendall, C.: Analysis of delta(15)N and delta(18)O to differentiate
826 NO(3)(-) sources in runoff at two watersheds in the Catskill Mountains of New York,
827 Water Resources Research, 38, 2002.
828 Casciotti, K. L., Sigman, D. M., Hastings, M. G., Bohlke, J. K., and Hilkert, A.:
829 Measurement of the oxygen isotopic composition of nitrate in seawater and freshwater
830 using the denitrifier method, Analytical Chemistry, 74, 4905-4912, 2002.
831 Cerco, C., Kim, S. C., and Noel, M. R.: The 2010 Chesapeake Bay Eutrophication
832 Model, A Report to the US Environmental Protection Agency and to the US Army Corps
833 of Engineer Baltimore District. US Army Engineer Research and Development Center,
834 Vicksburg, MD, (http://www.chesapeakebay.net/content/publications/cbp_26167.pdf),
835 2010. 2010.
836 Chesapeake Bay Program: CBP Water Quality Database (1984-present),
837 http://www.chesapeakebay.net/data/downloads/cbp_water_quality_database_1984_prese
838 nt, Accessd August 2013, 2013. 2013.
839 Cornwell, J. C., Glibert, P. M., and Owens, M. S.: Nutrient Fluxes from Sediments in the
840 San Francisco Bay Delta, Estuaries and Coasts, 37, 1120-1133, 2014.
841 Cornwell, J. C., Owens, M. S., Boynton, W. R., and Harris, L. A.: Sediment-Water
842 Nitrogen Exchange along the Potomac River Estuarine Salinity Gradient, Journal of
843 Coastal Research, 32, 776-787, 2016.
844 Crump, B. C. and Baross, J. A.: Particle-attached bacteria and heterotrophic plankton
845 associated with the Columbia River estuarine turbidity maxima, Marine Ecology Progress
846 Series, 138, 265-273, 1996.

847 Dawson, R. N. and Murphy, K. L.: Temperature dependency of biological denitrification,
848 Water Research, 6, 71-&, 1972.
849 Divers, M. T., Elliott, E. M., and Bain, D. J.: Quantification of Nitrate Sources to an
850 Urban Stream Using Dual Nitrate Isotopes, Environ. Sci. Technol., 48, 10580-10587,
851 2014.
852 Easterling, D. R., Meehl, G. A., Parmesan, C., Changnon, S. A., Karl, T. R., and Mearns,
853 L. O.: Climate extremes: Observations, modeling, and impacts, Science, 289, 2068-2074,
854 2000.
855 Elliott, A. J.: The circulation and salinity distribution of the upper Potomac estuary
856 Maryland USA, Chesapeake Science, 17, 141-147, 1976.
857 Elliott, A. J.: Observations of meteorologically induced circulation in Potomac estuary,
858 Estuarine and Coastal Marine Science, 6, 285-299, 1978.
859 Eyre, B. D. and Ferguson, A. J. P.: Benthic metabolism and nitrogen cycling in a
860 subtropical east Australian Estuary (Brunswick): Temporal variability and controlling
861 factors, Limnology and Oceanography, 50, 81-96, 2005.
862 Fawcett, S. E., Ward, B. B., Lomas, M. W., and Sigman, D. M.: Vertical decoupling of
863 nitrate assimilation and nitrification in the Sargasso Sea, Deep-Sea Research Part I-
864 Oceanographic Research Papers, 103, 64-72, 2015.
865 Filoso, S. and Palmer, M. A.: Assessing stream restoration effectiveness at reducing
866 nitrogen export to downstream waters, Ecological Applications, 21, 1989-2006, 2011.
867 Fisher, T. R., Gustafson, A. B., Sellner, K., Lacouture, R., Haas, L. W., Wetzel, R. L.,
868 Magnien, R., Everitt, D., Michaels, B., and Karrh, R.: Spatial and temporal variation of
869 resource limitation in Chesapeake Bay, Marine Biology, 133, 763-778, 1999.

870 Fogel, M. and Cifuentes, L.: Isotope fractionation during primary production, Plenum
871 Press, New York, 1993.
872 Gillooly, J. F., Brown, J. H., West, G. B., Savage, V. M., and Charnov, E. L.: Effects of
873 size and temperature on metabolic rate, Science, 293, 2248-2251, 2001.
874 Granger, J., Sigman, D. M., Lehmann, M. F., and Tortell, P. D.: Nitrogen and oxygen
875 isotope fractionation during dissimilatory nitrate reduction by denitrifying bacteria,
876 Limnology and Oceanography, 53, 2533-2545, 2008.
877 Granger, J., Sigman, D. M., Needoba, J. A., and Harrison, P. J.: Coupled nitrogen and
878 oxygen isotope fractionation of nitrate during assimilation by cultures of marine
879 phytoplankton, Limnology and Oceanography, 49, 1763-1773, 2004.
880 Hagy, J. D., Sanford, L. P., and Boynton, W. R.: Estimation of net physical transport and
881 hydraulic residence times for a coastal plain estuary using box models, Estuaries, 23,
882 328-340, 2000.
883 Hamdan, L. J. and Jonas, R. B.: Seasonal and interannual dynamics of free-living
884 bacterioplankton and microbially labile organic carbon along the salinity gradient of the
885 Potomac River, Estuaries and Coasts, 29, 40-53, 2006.
886 Harris, L. A. and Brush, M. J.: Bridging the gap between empirical and mechanistic
887 models of aquatic primary production with the metabolic theory of ecology: An example
888 from estuarine ecosystems, Ecological Modelling, 233, 83-89, 2012.
889 Hopkinson, C. S. and Vallino, J. J.: The relationships among mans activities in
890 watersheds and estuaries - a model of runoff effects on patterns of estuarine community
891 metabolism, Estuaries, 18, 598-621, 1995.

892 Horrigan, S. G., Montoya, J. P., Nevins, J. L., and McCarthy, J. J.: Natural isotopic
893 composition of dissolved inorganic nitrogen in the Chesapeake Bay, Estuarine Coastal
894 and Shelf Science, 30, 393-410, 1990.
895 IPCC: Climate Change 2007. The Physical Science Basis. Contribution of Working
896 Group I to the Fourth Assessment Report of the Intergovernmental Panel on Climate
897 Change, Cambridge University Press, Cambridge and New York, 2007.
898 Jaworski, N. A., Groffman, P. M., Keller, A. A., and Prager, J. C.: A watershed nitrogen
899 and phosphorus balance - the upper Potomac River basin, Estuaries, 15, 83-95, 1992.
900 Jordan, T. E., Cornwell, J. C., Boynton, W. R., and Anderson, J. T.: Changes in
901 phosphorus biogeochemistry along an estuarine salinity gradient: The iron conveyer belt,
902 Limnology and Oceanography, 53, 172-184, 2008.
903 Jordan, T. E., Weller, D. E., and Correll, D. L.: Sources of nutrient inputs to the Patuxent
904 River estuary, Estuaries, 26, 226-243, 2003.
905 Karrh, R., Romano, W., Garrison, S., Michael, B., Hall, M., Coyne, K., Reynolds, D., and
906 Ebersole, B.: Maryland Tributary Strategy Upper Potomac River Basin Summary Report
907 for 1985-2005 Data. Maryland Department of Natural Resources, 2007a.
908 Karrh, R., Romano, W., Raves-Golden, R., Tango, P., Garrison, S., Michael, B., Baldizar,
909 J., Trumbauer, C., Hall, M., Cole, B., Aadland, C., Trice, M., Coyne, K., Reynolds, D.,
910 Ebersole, B., and Karrh, L.: Maryland Tributary Strategy Lower Potomac River Basin
911 Summary Report for 1985-2005 Data. Maryland Department of Natural Resources,
912 2007b.

913 Karsh, K. L., Granger, J., Kritee, K., and Sigman, D. M.: Eukaryotic Assimilatory Nitrate
914 Reductase Fractionates N and O Isotopes with a Ratio near Unity, Environ. Sci. Technol.,
915 46, 5727-5735, 2012.
916 Karsh, K. L., Trull, T. W., Sigman, D. M., Thompson, P. A., and Granger, J.: The
917 contributions of nitrate uptake and efflux to isotope fractionation during algal nitrate
918 assimilation, Geochimica Et Cosmochimica Acta, 132, 391-412, 2014.
919 Kaushal, S. S. and Belt, K. T.: The urban watershed continuum: evolving spatial and
920 temporal dimensions, Urban Ecosystems, 15, 409-435, 2012.
921 Kaushal, S. S., Delaney-Newcomb, K., Findlay, S. E. G., Newcomer, T. A., Duan, S.,
922 Pennino, M. J., Sivirichi, G. M., Sides-Raley, A. M., Walbridge, M. R., and Belt, K. T.:
923 Longitudinal patterns in carbon and nitrogen fluxes and stream metabolism along an
924 urban watershed continuum, Biogeochemistry, DOI 10.1007/s10533-014-9979-9, 2014a.
925 Kaushal, S. S., Groffman, P. M., Band, L. E., Elliott, E. M., Shields, C. A., and Kendall,
926 C.: Tracking Nonpoint Source Nitrogen Pollution in Human-Impacted Watersheds,
927 Environ. Sci. Technol., 45, 8225-8232, 2011.
928 Kaushal, S. S., Likens, G. E., Jaworski, N. A., Pace, M. L., Sides, A. M., Seekell, D.,
929 Belt, K. T., Secor, D. H., and Wingate, R. L.: Rising stream and river temperatures in the
930 United States, Frontiers in Ecology and the Environment, 8, 461-466, 2010a.
931 Kaushal, S. S., Mayer, P. M., Vidon, P. G., Smith, R. M., Pennino, M. J., Duan, S.,
932 Newcomer, T. A., Welty, C., and Belt, K. T.: Land use and climate variability amplify
933 carbon, nutrient, and contaminant pulses: a review with management implications,
934 Journal of the American Water Resources Association, **50**, 585-614, 2014b.

935 Kaushal, S. S., McDowell, W. H., and Wollheim, W. M.: Tracking evolution of urban
936 biogeochemical cycles: past, present, and future, Biogeochemistry, 121, 1-21, 2014c.
937 Kaushal, S. S., Pace, M. L., Groffman, P. M., Band, L. E., Belt, K. T., Mayer, P. M., and
938 Welty, C.: Land use and climate variability amplify contaminant pulses, EOS, 91, 2010b.
939 Kemp, W. M., Sampou, P., Caffrey, J., Mayer, M., Henriksen, K., and Boynton, W. R.:
940 Ammonium recycling versus denitrification in Chesapeake Bay sediments, Limnology
941 and Oceanography, 35, 1545-1563, 1990.
942 Kendall, C., Elliott, E. M., and Wankel, S. D.: Tracing anthropogenic inputs of nitrogen
943 to ecosystems, Stable Isotopes in Ecology and Environmental Science, 2nd Edition, doi:
944 10.1002/9780470691854.ch12, 2007. 375-449, 2007.
945 Lehmann, M. F., Reichert, P., Bernasconi, S. M., Barbieri, A., and McKenzie, J. A.:
946 Modelling nitrogen and oxygen isotope fractionation during denitrification in a lacustrine
947 redox-transition zone, Geochimica Et Cosmochimica Acta, 67, 2529-2542, 2003.
948 Marconi, D., Weigand, M. A., Rafter, P. A., McIlvin, M. R., Forbes, M., Casciotti, K. L.,
949 and Sigman, D. M.: Nitrate isotope distributions on the US GEOTRACES North Atlantic
950 cross-basin section: Signals of polar nitrate sources and low latitude nitrogen cycling,
951 Marine Chemistry, 177, 143-156, 2015.
952 Mariotti, A., Germon, J. C., Hubert, P., Kaiser, P., Letolle, R., Tardieux, A., and
953 Tardieux, P.: Experimental-determination of nitrogen kinetic isotope fractionation - some
954 principles - illustration for the denitrification and nitrification processes, Plant and Soil,
955 62, 413-430, 1981.

Mayer, B., Bollwerk, S. M., Mansfeldt, T., Hutter, B., and Veizer, J.: The oxygen isotope composition of nitrate generated by nitrification in acid forest floors, Geochimica Et Cosmochimica Acta, 65, 2743-2756, 2001.

Mayer, B., Boyer, E. W., Goodale, C., Jaworski, N. A., Van Breemen, N., Howarth, R. W., Seitzinger, S., Billen, G., Lajtha, L. J., Nosal, M., and Paustian, K.: Sources of nitrate in rivers draining sixteen watersheds in the northeastern US: Isotopic constraints, Biogeochemistry, 57, 171-197, 2002.

Middelburg, J. J. and Nieuwenhuize, J.: Nitrogen isotope tracing of dissolved inorganic nitrogen behaviour in tidal estuaries, Estuarine Coastal and Shelf Science, 53, 385-391, 2001.

Middelburg, J. J. and Nieuwenhuize, J.: Nitrogen uptake by heterotrophic bacteria and phytoplankton in the nitrate-rich Thames estuary, Marine Ecology Progress Series, 203, 13-21, 2000.

Milliman, J. D., Shen, H. T., Yang, Z. S., and Meade, R. H.: Transport and deposition of river sediment in the changjiang estuary and adjacent continental-shelf, Continental Shelf Research, 4, 37-45, 1985.

Nixon, S. W., Ammerman, J. W., Atkinson, L. P., Berounsky, V. M., Billen, G., Boicourt, W. C., Boynton, W. R., Church, T. M., Ditoro, D. M., Elmgren, R., Garber, J. H., Giblin, A. E., Jahnke, R. A., Owens, N. J. P., Pilson, M. E. Q., and Seitzinger, S. P.: The fate of nitrogen and phosphorus at the land sea margin of the North Atlantic Ocean, Biogeochemistry, 35, 141-180, 1996.

977 Nowicki, B. L.: The effect of temperature, oxygen, salinity, and nutrient enrichment on
978 estuarine denitrification rates measured with a modified nitrogen gas flux technique,
979 Estuarine Coastal and Shelf Science, 38, 137-156, 1994.
980 Oczkowski, A., Nixon, S., Henry, K., DiMilla, P., Pilson, M., Granger, S., Buckley, B.,
981 Thornber, C., McKinney, R., and Chaves, J.: Distribution and trophic importance of
982 anthropogenic nitrogen in Narragansett Bay: An assessment using stable isotopes,
983 Estuaries and Coasts, 31, 53-69, 2008.
984 Officer, C. B.: Box models revisited. In: Estuarine and wetland processes, with emphasis
985 on modeling, Hamilton, P. and Macdonald, K. B. (Eds.), Plenum Press, New York and
986 London, 1980.
987 Paerl, H. W., Valdes, L. M., Piehler, M. F., and Stow, C. A.: Assessing the effects of
988 nutrient management in an estuary experiencing climatic change: The Neuse River
989 Estuary, North Carolina, Environ. Manage., 37, 422-436, 2006.
990 Parnell, A. C., Inger, R., Bearhop, S., and Jackson, A. L.: Source Partitioning Using
991 Stable Isotopes: Coping with Too Much Variation, Plos One, 5, 2010.
992 Parnell, A. C., Phillips, D. L., Bearhop, S., Semmens, B. X., Ward, E. J., Moore, J. W.,
993 Jackson, A. L., Grey, J., Kelly, D. J., and Inger, R.: Bayesian stable isotope mixing
994 models, Environmetrics, 24, 387-399, 2013.
995 Petrone, K. C.: Catchment export of carbon, nitrogen, and phosphorus across an agro-
996 urban land use gradient, Swan-Canning River system, southwestern Australia, Journal of
997 Geophysical Research-Biogeosciences, G01016 2010.

998 Pfenning, K. S. and McMahon, P. B.: Effect of nitrate, organic carbon, and temperature
999 on potential denitrification rates in nitrate-rich riverbed sediments, Journal of Hydrology,
1000 187, 283-295, 1997.
1001 Pritchard, D. W.: The dynamic structure of a coastal plain estuary, Journal of Marine
1002 Research, 15, 33-42, 1956.
1003 R Development Core Team: http://www.R-project.org, 2013.
1004 Rafter, P. A., DiFiore, P. J., and Sigman, D. M.: Coupled nitrate nitrogen and oxygen
1005 isotopes and organic matter remineralization in the Southern and Pacific Oceans, Journal
1006 of Geophysical Research-Oceans, 118, 4781-4794, 2013.
1007 Sanford, L. P., Suttles, S. E., and Halka, J. P.: Reconsidering the physics of the
1008 Chesapeake Bay estuarine turbidity maximum, Estuaries, 24, 655-669, 2001.
1009 Saunders, M. A. and Lea, A. S.: Large contribution of sea surface warming to recent
1010 increase in Atlantic hurricane activity, Nature, 451, 557-U553, 2008.
1011 Sigman, D. M., Casciotti, K. L., Andreani, M., Barford, C., Galanter, M., and Bohlke, J.
1012 K.: A bacterial method for the nitrogen isotopic analysis of nitrate in seawater and
1013 freshwater, Analytical Chemistry, 73, 4145-4153, 2001.
1014 Smart, S. M., Fawcett, S. E., Thomalla, S. J., Weigand, M. A., Reason, C. J. C., and
1015 Sigman, D. M.: Isotopic evidence for nitrification in the Antarctic winter mixed layer,
1016 Global Biogeochemical Cycles, 29, 427-445, 2015.
1017 Testa, J. M., Kemp, W. M., Boynton, W. R., and Hagy, J. D.: Long-Term Changes in
1018 Water Quality and Productivity in the Patuxent River Estuary: 1985 to 2003, Estuaries
1019 and Coasts, 31, 1021-1037, 2008.

U.S. EPA: http://catalog.data.gov/dataset/concentrated-animal-feeding-operations-cafos-per-county-downloadable-package-us-2013-us-epa, last access: September 22, 2016 2016.

US-EPA: http://cfpub.epa.gov/npdes/cwa.cfm, 1972.

US-EPA: http://cfpub.epa.gov/npdes/, 2009.

US-EPA: U.S. Environmental Protection Agency. National Pollutant Discharge Elimination System (NPDES) Stormwater Program, 2011. 2011.

USGS: US Geological Survey Surface Water Data. http://waterdata.usgs.gov/md/nwis/uv?01646500. Accessed June 2014, 2014. 2014.

Vavilin, V. A.: Describing a Kinetic Effect of Fractionation of Stable Nitrogen Isotopes in Nitrification Process, Water Resources, 41, 325-329, 2014.

Vavilin, V. A., Rytov, S. V., and Lokshina, L. Y.: Non-linear dynamics of nitrogen isotopic signature based on biological kinetic model of uptake and assimilation of ammonium, nitrate and urea by a marine diatom, Ecological Modelling, 279, 45-53, 2014.

Vitousek, P. M., Aber, J. D., Howarth, R. W., Likens, G. E., Matson, P. A., Schindler, D. W., Schlesinger, W. H., and Tilman, D.: Human alteration of the global nitrogen cycle: Sources and consequences, Ecological Applications, 7, 737-750, 1997.

Wang, S. Q., Tang, C. Y., Song, X. F., Yuan, R. Q., Wang, Q. X., and Zhang, Y. H.: Using major ions and delta N-15-NO3- to identify nitrate sources and fate in an alluvial aquifer of the Baiyangdian lake watershed, North China Plain, Environmental Science-Processes & Impacts, 15, 1430-1443, 2013.

Wankel, S. D., Kendall, C., Francis, C. A., and Paytan, A.: Nitrogen sources and cycling in the San Francisco Bay Estuary: A nitrate dual isotopic composition approach, Limnology and Oceanography, 51, 1654-1664, 2006.

Waser, N. A., Yin, K. D., Yu, Z. M., Tada, K., Harrison, P. J., Turpin, D. H., and Calvert, S. E.: Nitrogen isotope fractionation during nitrate, ammonium and urea uptake by marine diatoms and coccolithophores under various conditions of N availability, Marine Ecology Progress Series, 169, 29-41, 1998a.

Waser, N. A. D., Harrison, P. J., Nielsen, B., Calvert, S. E., and Turpin, D. H.: Nitrogen isotope fractionation during the uptake and assimilation of nitrate, nitrite, ammonium, and urea by a marine diatom, Limnology and Oceanography, 43, 215-224, 1998b.

Wiegert, R. G. and Penaslado, E.: Nitrogen-pulsed systems on the coast of northwest Spain, Estuaries, 18, 622-635, 1995.

Xue, D. M., De Baets, B., Van Cleemput, O., Hennessy, C., Berglund, M., and Boeckx, P.: Use of a Bayesian isotope mixing model to estimate proportional contributions of multiple nitrate sources in surface water, Environmental Pollution, 161, 43-49, 2012.

Yang, Y. Y. and Toor, G. S.: delta N-15 and delta O-18 Reveal the Sources of Nitrate-Nitrogen in Urban Residential Stormwater Runoff, Environ. Sci. Technol., 50, 2881-2889, 2016.

1065

1066

1067

1068

1069

1070

1071

1072

1073

1074

1075 Table 1. Seasonal comparison of N and C inputs, exports, and losses along the Potomac River Estuary (mean ± standard error).

	Nutrient	Total Inputs (kg/day)	% of Inputs from Blue Plains*	Net Export (kg/day)	% of Blue Plains Inputs Exported	Net Loss in Load along Estuary, Box 1 to 6 (kg/day)	% Net Loss in Load along Estuary, Box 1 to 6	Net Loss in Load along Estuary, Box 1 to 5 (kg/day)	% Net Loss in Load along Estuary, Box 1 to 5	Net Loads from Bay to Estuary (kg/day)
Winter	TN	49150 ± 30323	10 ± 13	19844 ± 13728	3.7 ± NA	27369 ± 14597	54 ± 40	16426 ± 9509	28 ± 25	473 ± 414
Spring	TN	135317 ± 14614	8 ± 0.8	68431 ± 48060	71 ± 20	49672 ± 52116	36 ± 43	29515 ± 32908	26 ± 21	-127 ± 480
Summer	TN	13888 ± 596	38 ± 3	4853 ± 8326	19 ± 11	7155 ± 8370	75 ± 75	5739 ± 1832	44 ± 21	380 ± 164
Fall	TN	15334 ± 3700	47 ± 13	-1613 ± 12124	18 ± 10	15364 ± 12548	112 ± 95	4140 ± 6607	30 ± 43	264 ± 290
Winter	NO_3^-	37749 ± 23574	5.7 ± 4.6	2080 ± 6235	3 ± NA	31791 ± 7417	93 ± 29	26299 ± 10069	74 ± 33	32 ± 58
Spring	NO_3^-	95395 ± 10416	7.4 ± 0.6	30039 ± 161747	52 ± 70	40206 ± 161977	60 ± 187	30998 ± 26791	46 ± 34	8 ± 109
Summer	NO_3^-	7066 ± 364	49 ± 6.3	105 ± 4130	17 ± 2	5166 ± 4143	96 ± 141	4223 ± 763	77 ± 19	11 ± 10
Fall	NO_3^-	10526 ± 3006	53 ± 18.2	-204 ± 6278	13 ± 35	7291 ± 6812	108 ± 181	5637 ± 6817	85 ± 122	13 ± 35
Winter	$\delta^{15}N\text{-}NO_3^-$	130 ± 10	4 ± 0.4	4 ± NA	2.7 ± NA	130 ± NA	97 ± NA	77 ± NA	68 ± NA	86 ± NA
Spring	$\delta^{15}N\text{-}NO_3^-$	374 ± 3	7 ± 0.1	170 ± 547	52 ± 136	88 ± 547	48 ± 136	42 ± 71	26 ± 31	-412 ± 1471
Summer	$\delta^{15}N\text{-}NO_3^-$	30 ± 1	53 ± 1.6	5 ± 1	17 ± 3	27 ± 1	83 ± 3	18 ± 1	83 ± 3	NA
Fall	$\delta^{15}N\text{-}NO_3^-$	40 ± 5	55 ± 5.8	7 ± 8	13 ± 68	26 ± 8	87 ± 105	26 ± 13	87 ± 105	NA

1076 TN = Total Nitrogen. NA – indicates there was only one month with data for that season and thus no S.E. value.
1077 *Blue Plains is a wastewater treatment plant.

Table 2. Comparison of mean (± standard error) seasonal discharge and residence time within the Potomac River Estuary

	Mean Discharge (m^3/s)	Mean Residence time (days)
Winter	187 ± 60	26 ± 18
Spring	545 ± 214	57 ± 36
Summer	81 ± 29	129 ± 85
Fall	81 ± 27	196 ± 102

Data is based on discharge and box model results for the period from April 2010 to March 2011.

Figures

Figure 1. Map showing the Potomac River sampling stations (black diamond) and the location of the Blue Plains Wastewater Treatment plant (WWTP, black X) just south of Washington D.C., within the Chesapeake Bay watershed. The larger figure shows the location of monthly extensive synoptic surveys sites and the smaller figure on upper left shows the locations of the shorter intensive synoptic surveys. The larger figure also shows the location for the historical Maryland DNR surface water sampling sites.

Figure 2. Plot of the Potomac Estuary depth with distance down-estuary, with the Blue Plains wastewater treatment plant at distance zero, showing the location of the 6 boxes used in the box model calculations.

Figure 3. Longitudinal patterns in Potomac River Estuary: (a) mean annual dissolved inorganic nitrogen (DIN) and total organic nitrogen (TON) spanning 1997 to 2005, (b) mean seasonal DIN before year 2000 (1994 to 1999), and post 2000 (2001 to 2012), and (c) mean (1994 to 2012) seasonal molar N:P ratio (DIN/PO_4^{-3}), with salinity averaged from all seasons (1984 to 2008). Note: errors bars are provided, but S.E. is relatively small compared to concentrations. This data was obtained from the Maryland DNR and the Chesapeake Bay Program Data Hub.

Figure 4. Comparison of NO_3^- *vs*. dissolved organic carbon (DOC). N and C data was obtained from the Maryland DNR and the Chesapeake Bay Program Data Hub for this study period (2010-2012).

Figure 5. Trends in (a) $\delta^{15}N\text{-}NO_3^-$, (b) $\delta^{18}O\text{-}NO_3^-$, and (c) percent contribution of nitrate from wastewater, the atmospheric, and nitrification, based on isotope mixing model, with distance down-estuary from wastewater treatment plant input. Error bars are standard errors of the mean. N = 1 for winter, N = 3 for spring and fall, and N = 2 for summer.

Figure 6. (a) Plot of $\delta^{15}N\text{-}NO_3^-$ *vs.* $\delta^{18}O\text{-}NO_3^-$ of nitrate from effluent water samples and Potomac River Estuary samples, showing samples from different locations along the estuary; the grey arrow indicates the 2:1 relationship characteristic for denitrification; and (b) Same plot as (a), but seasonally and without the effluent or wastewater outfall values. Not included in these plots is the box indicating the region where atmospheric nitrate samples generally lie, from -10 to +15 for $\delta^{15}N\text{-}NO_3^-$ and from 60 to 100 for $\delta^{18}O\text{-}NO_3^-$.

Figure 7. Comparison of salinity *vs.* (a) NO_3^-, (b) $\delta^{15}N\text{-}NO_3^-$ and (c) $\delta^{18}O\text{-}NO_3^-$. Mixing lines connect the mean NO_3^- concentration or isotope values at the lowest and highest salinity values. Error bars are standard errors of the mean. For panel (a), N = 3 for all seasons, for panels (b) and (c), N = 1 for winter, N = 3 for spring and fall, and N = 2 for summer. Mixing line equations for NO_3^- concentrations and isotopes were obtained from Middelburg and Nieuwenhuize (2001). NO_3^- data was obtained from the Maryland DNR and the Chesapeake Bay Program Data Hub, covering spring 2010 to spring 2011, the same dates as the NO_3^- isotope data.

Figure 8. Comparing the TN fluxes along the Potomac River Estuary estimated from the Box Model used in this study and from the results from the Chesapeake Bay nutrient model.

Figure 9. Correlation between the fluxes estimated from the Box Model used in this study and the Chesapeake Bay nutrient model.

Figure 10. Seasonal Box Model results showing how (a) TN, (b) NO_3^-, and (c) $\delta^{15}N\text{-}NO_3^-$ loads vary down-estuary. Error bars are standard errors of the mean. For panels (a) and (b), N = 3 for all seasons. For panel (c), N = 1 for winter, N = 3 for spring and fall, and N = 2 for summer. TN and NO_3^- data was obtained from the Maryland DNR and the Chesapeake Bay Program Data Hub.

1159 Figure 1.

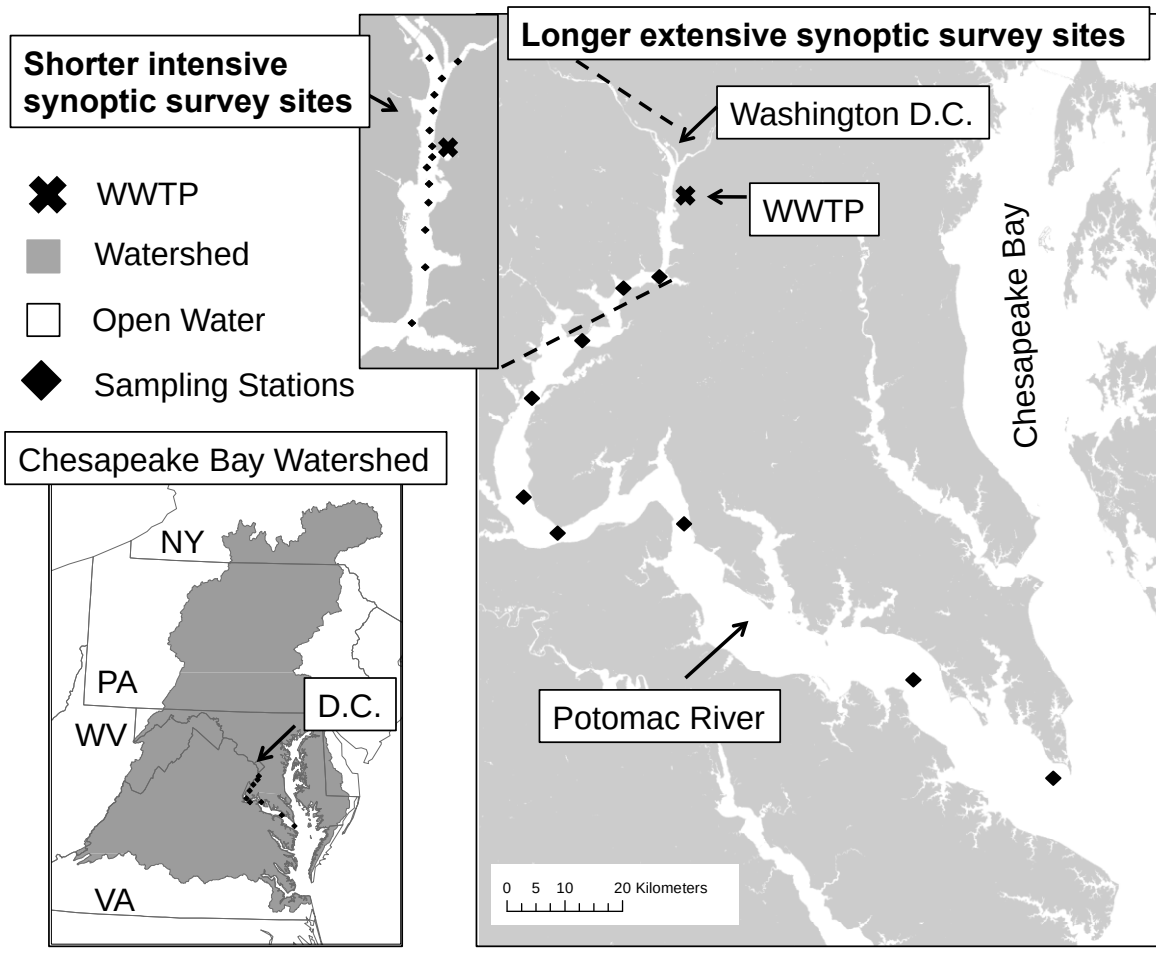

1160
1161

1162

1163

1164

1165

1166

1167

1168

1169

1170

1171 Figure 2.

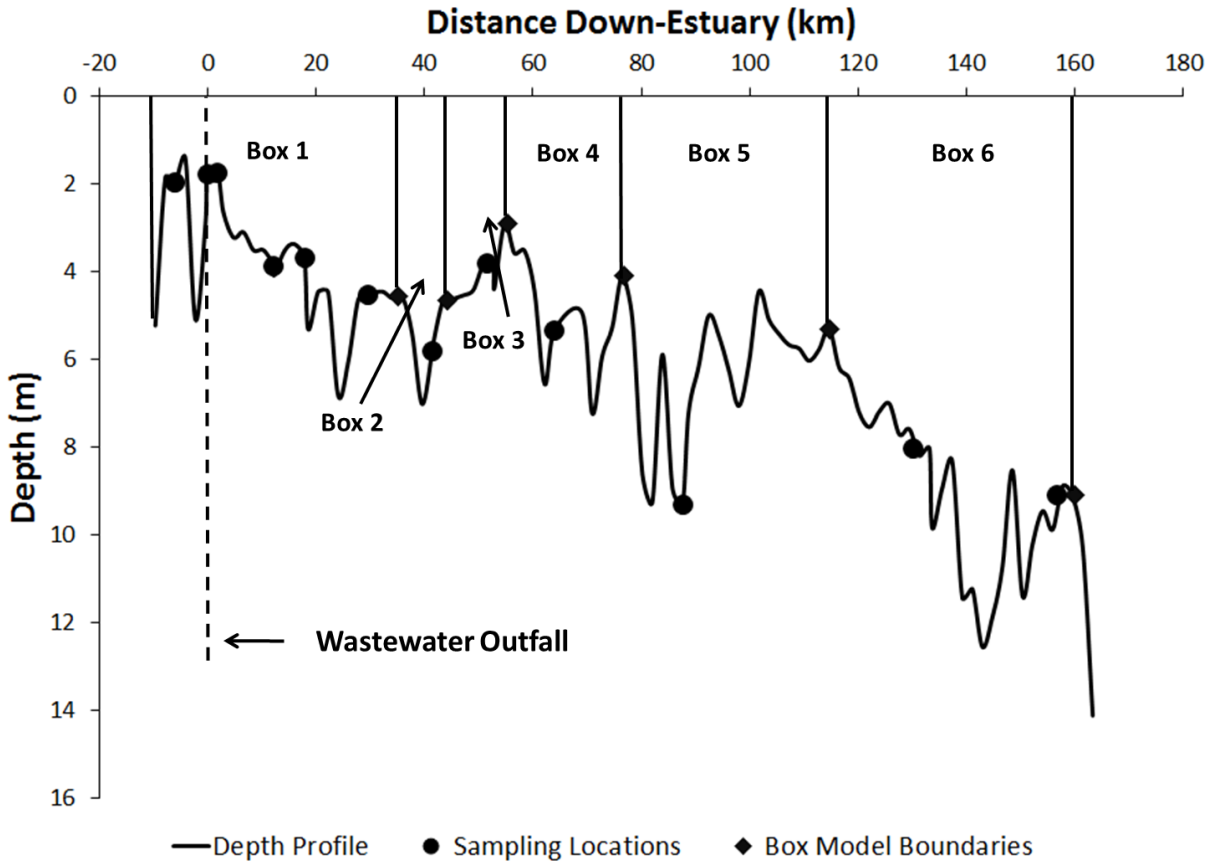

1172
1173
1174
1175
1176
1177
1178
1179
1180
1181
1182
1183
1184
1185
1186
1187
1188
1189

1190 Figure 3.

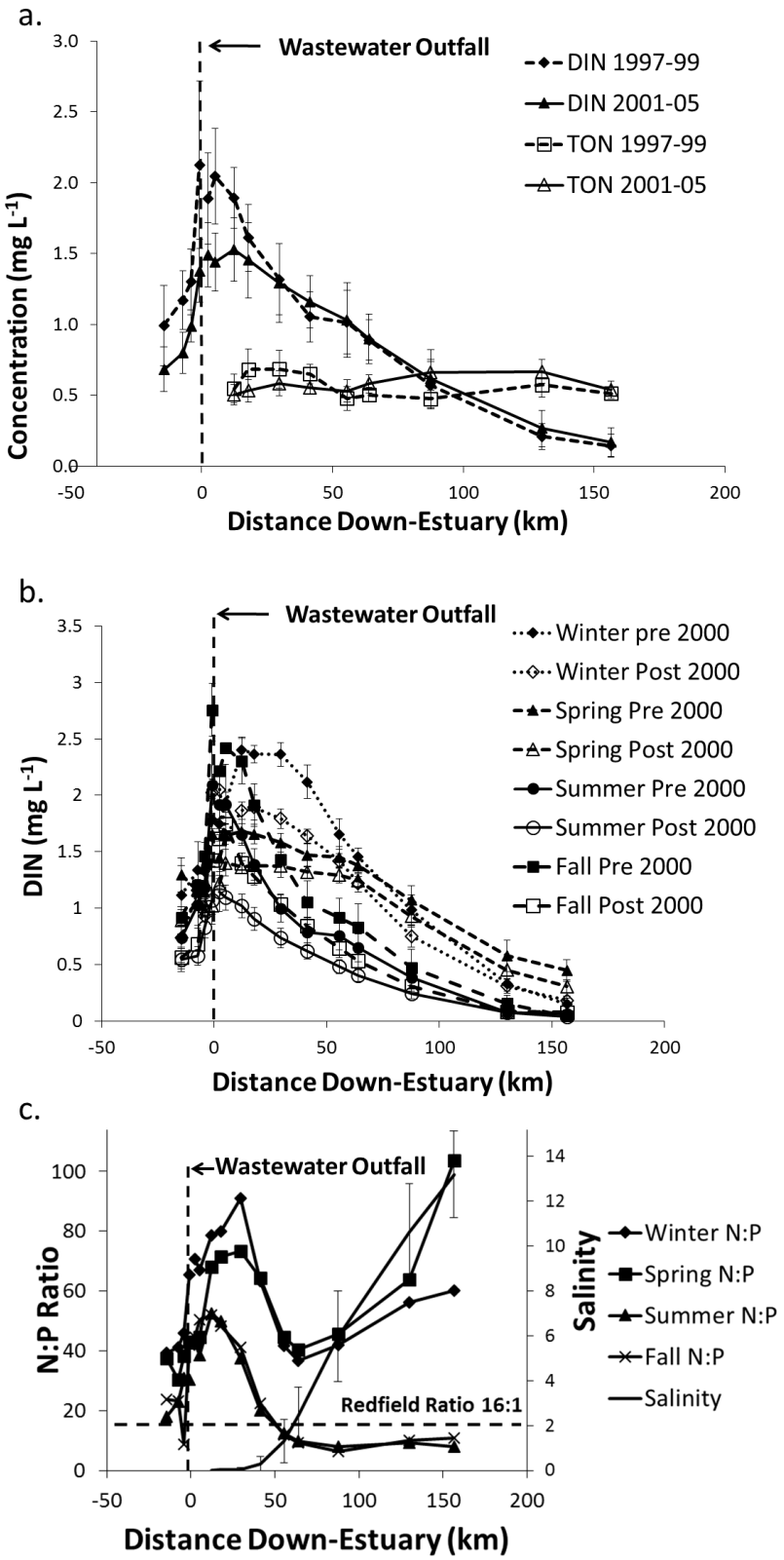

1191

Figure 4.

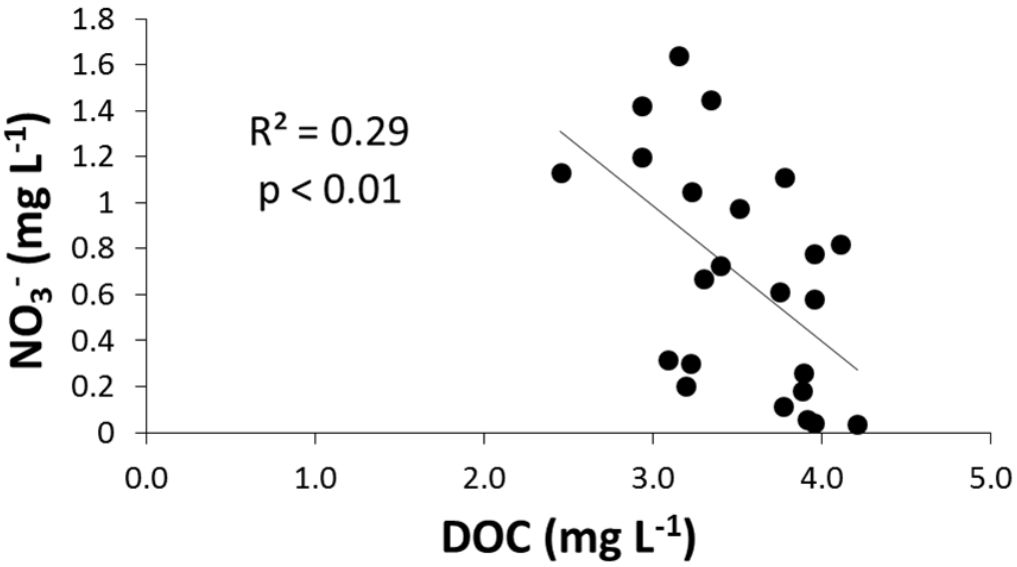
1.8
1.6
1.4
1.2
1
0.8
0.6
0.4
0.2
0
NO_3^- (mg L^{-1})
R^2 = 0.29
p < 0.01
0.0
1.0
2.0
3.0
4.0
5.0
DOC (mg L^{-1})

1223 Figure 5.

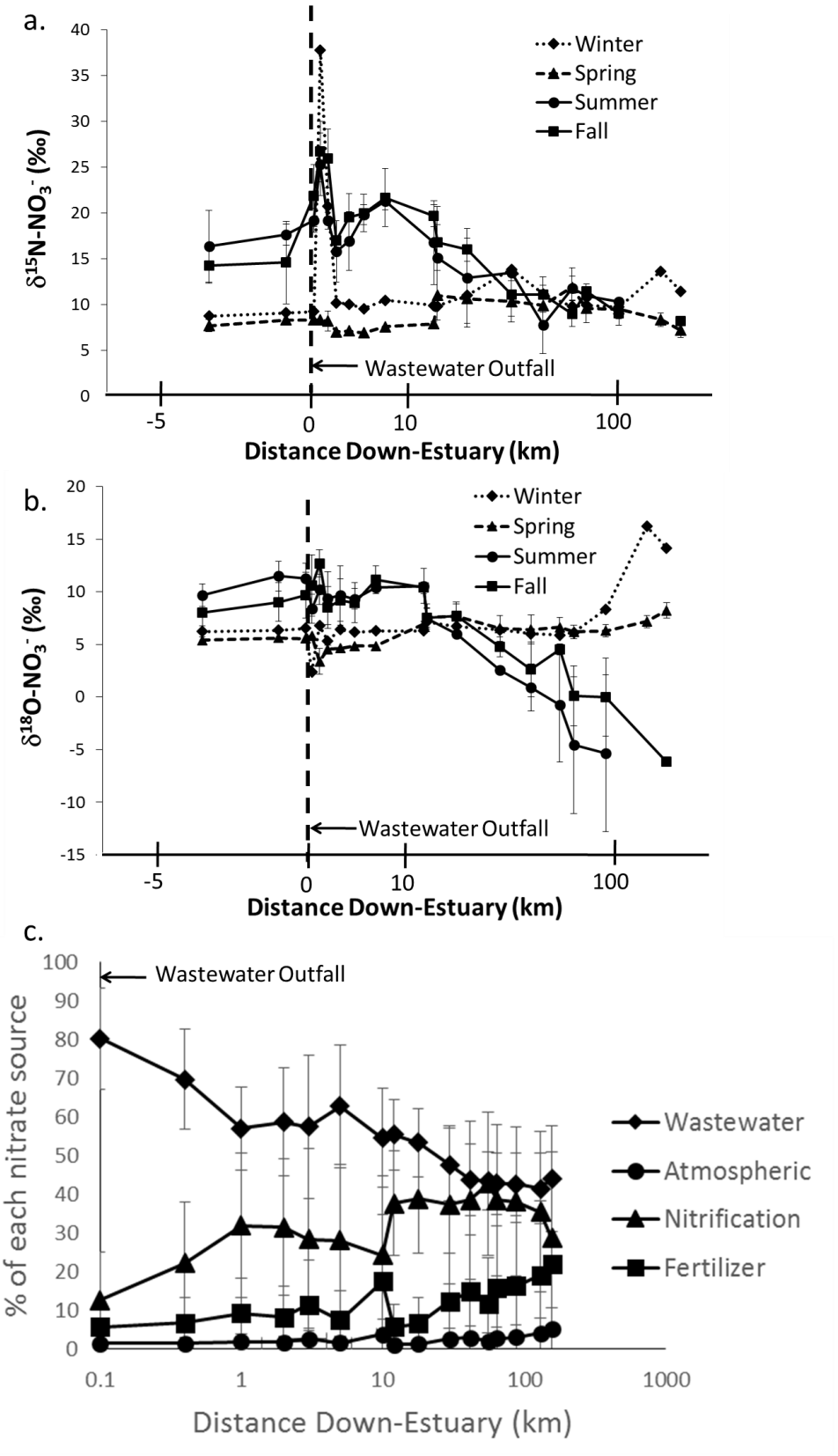

1224

1225 Figure 6.

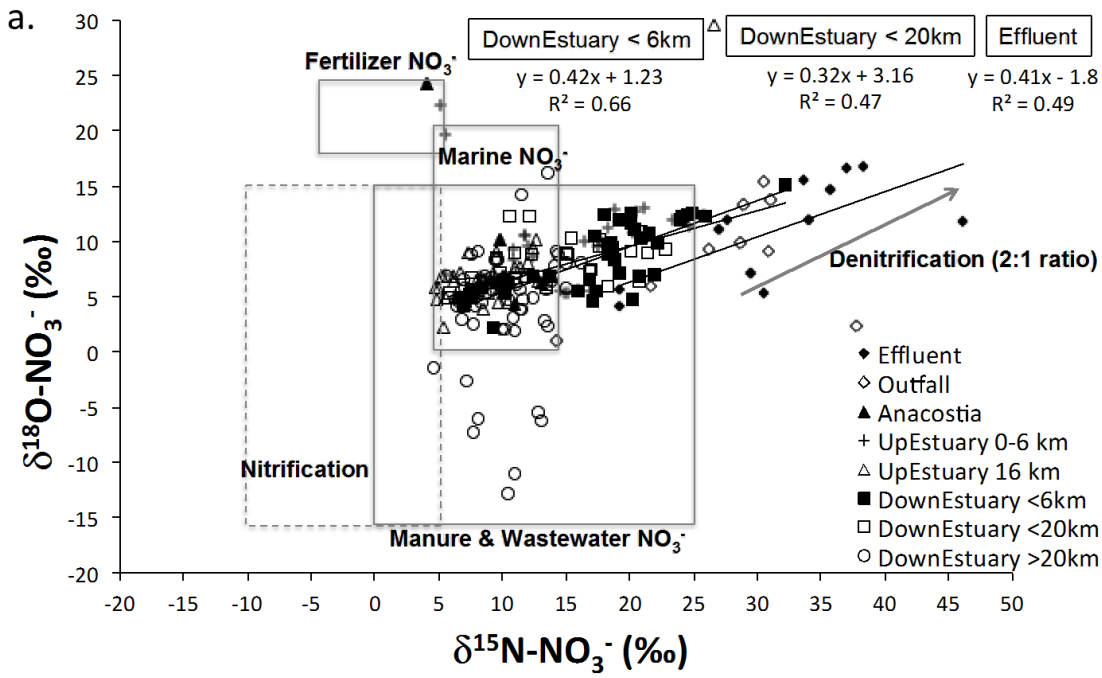

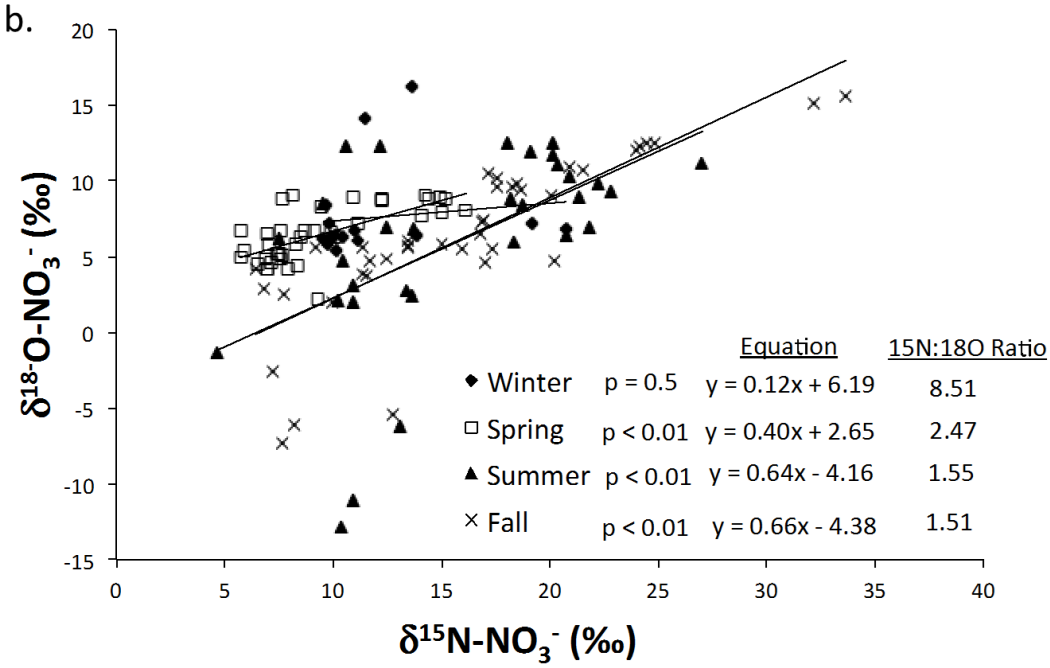

1226
1227
1228
1229
1230
1231
1232
1233
1234

1235 Figure 7.

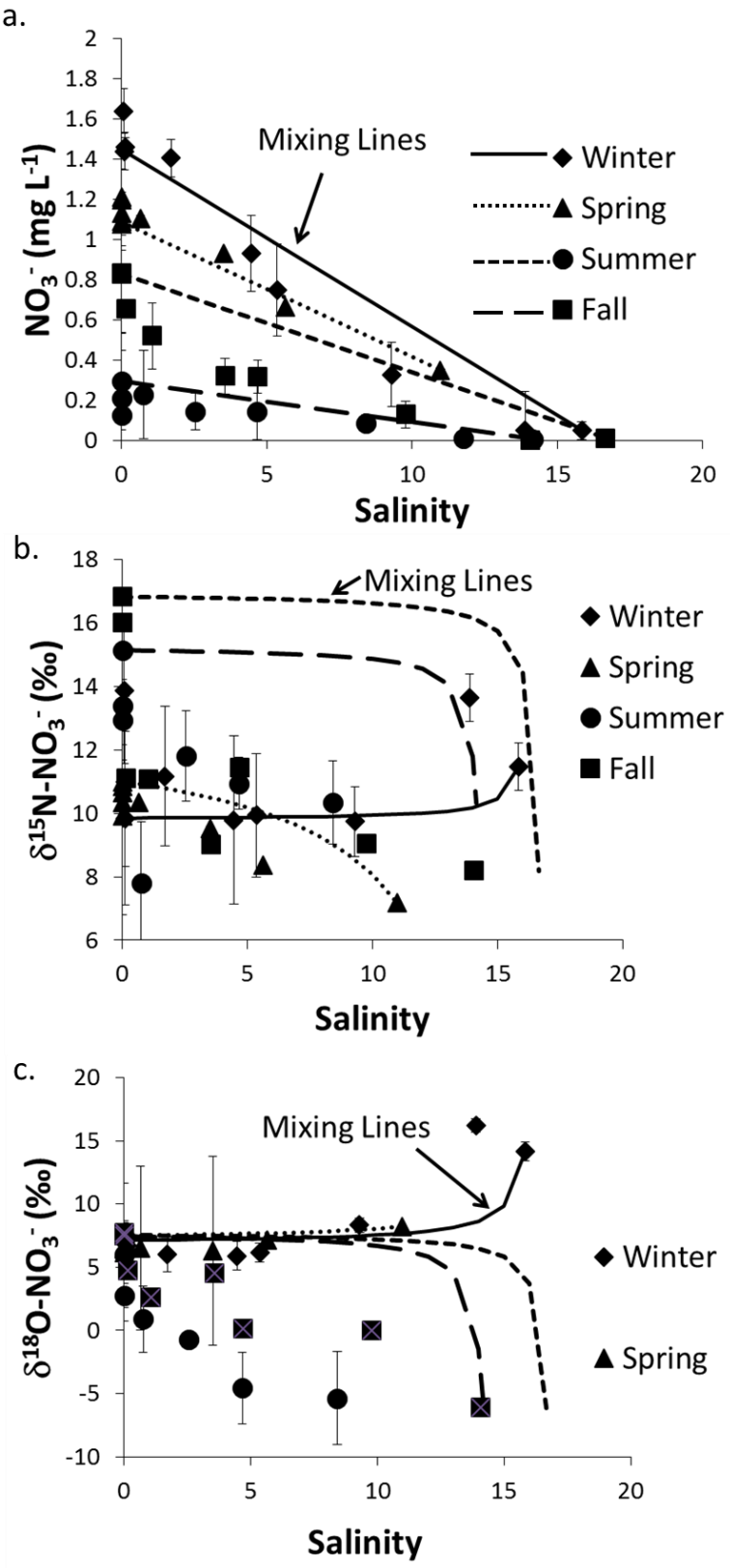

1236
1237

Figure 8.

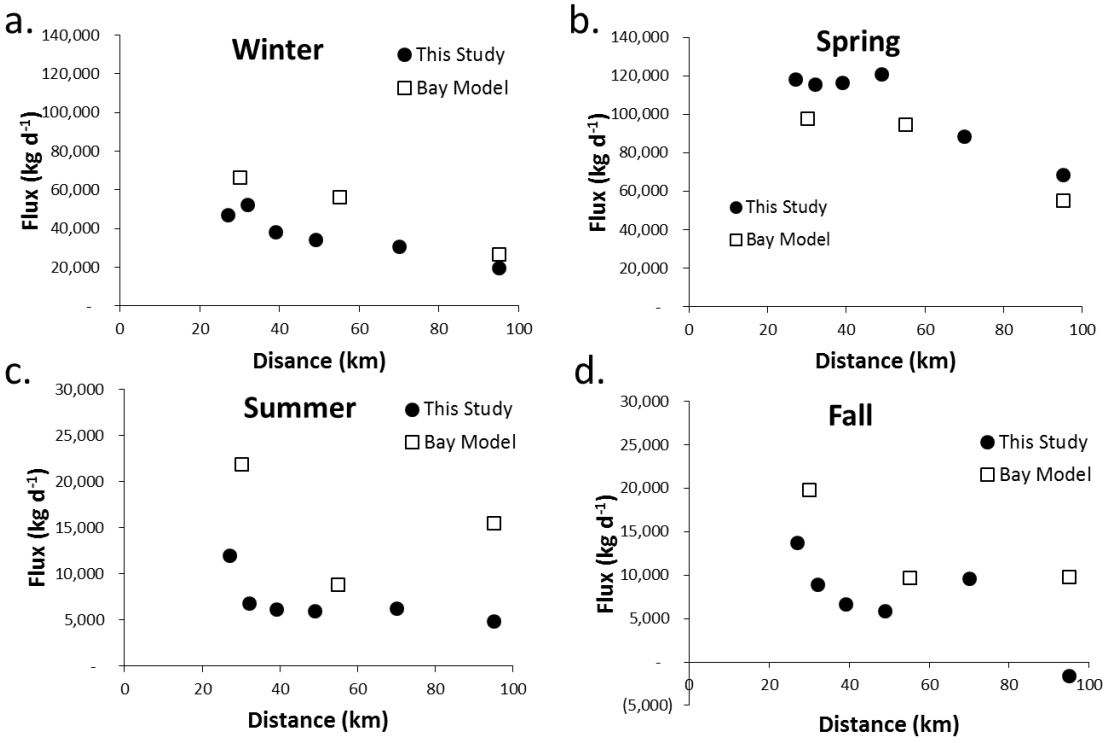
a.
Winter
This Study
Bay Model
Flux (kg d-1)
Disance (km)
b.
Spring
This Study
Bay Model
Flux (kg d-1)
Distance (km)
c.
Summer
This Study
Bay Model
Flux (kg d-1)
Distance (km)
d.
Fall
This Study
Bay Model
Flux (kg d-1)
Distance (km)

Figure 9.

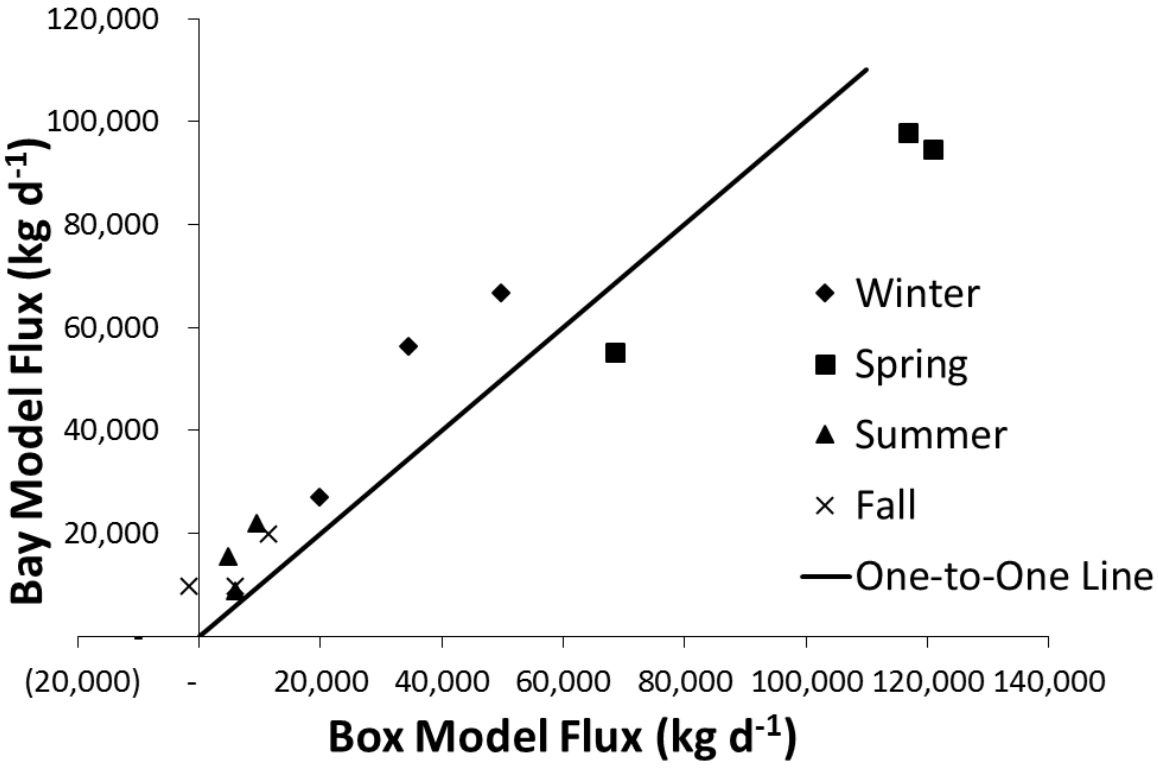
120,000
100,000
80,000
60,000
40,000
20,000
Bay Model Flux (kg d-1)
(20,000)
-
20,000
40,000
60,000
80,000
100,000
120,000
140,000
Box Model Flux (kg d-1)
Winter
Spring
Summer
Fall
One-to-One Line

1291 Figure 10.

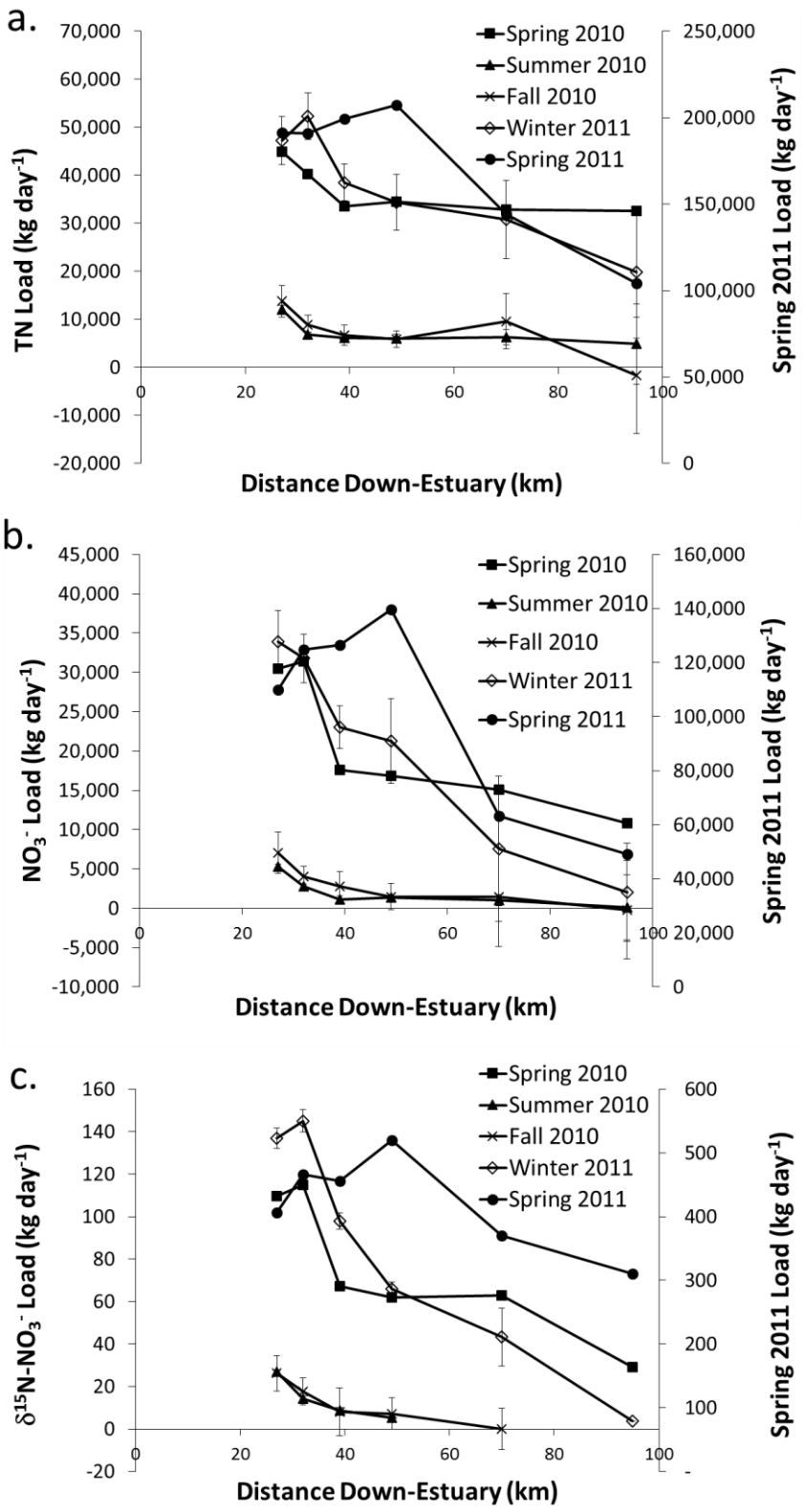

1292